Diploma thesis

Evaluation of intracytoplasmic hyaline inclusions as markers for malignancy in hepatocellular liver tumors

submitted by

Oliver Scheiber

attaining the academic degree

Doctor medicinae universae

(Dr. med. univ.)

at the

Medical University of Graz

conducted at the

Diagnostics & Research Institute of Pathology

under supervision of

Univ.-Prof.in Dr.in med.univ. Carolin Lackner

and

Priv.-Doz.in Dr.in med.univ. Ariane Aigelsreiter

Graz, July 26th, 2018

Affidavit

I hereby declare that the following diploma thesis has been written only by the undersigned and without any assistance from third parties. Furthermore, I confirm that no sources have been used in the preparation of this thesis other than those indicated in the thesis itself.

Graz, July 26th, 2018 Oliver Scheiber eh

Acknowledgements

First, I would like to thank Univ.-Prof.in Dr.in Carolin Lackner for giving me the chance to get unique insights in hepatopathology. Thank you for spending hours with me in the front of the multiheaded microscope and for sharing your huge knowledge. Thank you for your patient explanations and helpful advices that finally led to this diploma thesis. Moreover, I want to address thanks to Priv.-Doz.in Dr.in Ariane Aigelsreiter for co-supervising my diploma thesis.

Additionally, I owe sincere gratitude to Brigitte Tessaro for all concerns in immunohistochemistry. Thank you for your excellent support.

Moreover, I want to extend special thanks to my whole family for supporting me in every sense. Thank you for giving me the chance to study.

Finally, I want to thank my girlfriend Mirjam for her patience with me during tough hours.

Abstract

Background and aims: Hyaline bodies, Mallory-Denk bodies (MDB) and intracellular hyaline bodies (IHB), may occur as a consequence of a variety of stresses in cells with hepatocellular differentiation. MDB have been described in benign liver diseases as well as in benign and malignant tumors of the liver. In contrast, IHB have only been observed in hepatocellular carcinomas (HCC). Thus IHB may serve as morphological tumor markers. Therefore, the aim of this study is to analyze occurrence of these intracytoplasmic hyaline inclusions in precursor lesions of HCC in cirrhotic and non-cirrhotic liver.

Patients, materials and methods: 61 precursor lesions, 11 large cell changes, 10 small cell changes, 20 low-grade dysplastic nodules (LGDN), 13 high-grade dysplastic nodules (HGDN), 7 HGDN with HCC foci, 90 HCC and additionally, benign tumors with malignant potential, 23 focal nodular hyperplasias (FNH) and 13 hepatocellular adenomas (HCA), were histologically as well as immunohistochemically analyzed and occurrence of MDB and IHB was correlated with histological diagnosis by statistical analysis.

Results: In our study, MDB were identified in all precursor lesions in cirrhotic liver and in regenerative nodules of cirrhosis. Highest relative frequencies have been observed in HGDN (53.8%) and in HGDN with foci of HCC (71.4%). In contrast, IHB have exclusively been detected in 31.1% of HCC and in 28.6% of HCC foci within HGDN but in none of the other precursor lesions of HCC.

Conclusions: IHB and MDB can be easily and inexpensively identified on H&E histology. Occurrence of IHB in tumors of the liver with hepatocellular differentiation correlates strictly with malignant hepatocellular lesions and thus IHB are able to support diagnosis of HCC as a tumor marker whereas MDB in a dysplastic nodule may suggest high-grade dysplasia.

Zusammenfassung

Hintergrund und Ziele: Hyaline Körper, Mallory-Denk-Körper (MDB) und intrazelluläre hyaline Körper (IHB), können bei unterschiedlichen Arten von Stress in hepatozellulär differenzierten Zellen auftreten. MDB wurden sowohl in benignen Lebererkrankungen als auch in benignen und malignen Tumoren der Leber beschrieben. Im Gegensatz dazu wurden IHB nur in hepatozellulären Karzinomen (HCC) beobachtet. IHB könnten deshalb als morphologische Tumormarker dienen. Das Ziel dieser Studie ist es deshalb, das Auftreten dieser intrazytoplasmatischen hyalinen Inklusionen in Vorläuferläsionen des HCC in zirrhotischer und nicht-zirrhotischer Leber zu untersuchen.

Patientinnen und Patienten, Material und Methoden: Es wurden 61 Vorläuferläsionen, 11 großzellige Dysplasien, 10 kleinzellige Dysplasien, 20 niedriggradig dysplastische Knoten (LGDN), 13 hochgradig dysplastische Knoten (HGDN), 7 HGDN mit HCC-Foci, 90 HCC und zusätzlich benigne Tumore, 23 fokale noduläre Hyperplasien (FNH) und 13 hepatozelluläre Adenome (HCA), in denen HCC entstehen können, histologisch und immunhistochemisch untersucht und das Auftreten von MDB und IHB mit der histologischen Diagnose mittels statistischer Methoden korreliert.

Ergebnisse: In unserer Studie wurden MDB in allen Vorläuferläsionen der zirrhotischen Leber und in Regeneratknoten der Zirrhose identifiziert. Die höchsten relativen Häufigkeiten wurden in HGDN (53.8%) und in HGDN mit HCC-Foci (71.4%) beobachtet. Im Gegensatz dazu wurden IHB ausschließlich in 31.1% der HCC und in 28.6% der HCC-Foci innerhalb von HGDN, jedoch in keiner anderen Form von Vorläuferläsionen des HCC, identifizert.

Schlussfolgerungen: IHB und MDB können am H&E-Schnitt einfach und kostengünstig identifiziert werden. Das Auftreten von IHB in hepatozellulär differenzierten Tumoren der Leber korreliert strikt mit malignen hepatozellulären Läsionen und unterstützt somit als Tumormarker die Diagnose eines HCC, wohingegen MDB in einem dysplastischen Knoten auf eine hochgradige Dysplasie hinweisen können.

Table of Contents

Index of Abbreviations

AASLD	American Association for the Study of Liver Diseases
AEC	3-amino-9-ethylcarbazole
AFP	Alpha-fetoprotein
ALD	Alcoholic liver disease
ASH	Alcoholic steatohepatitis
BCLC	Barcelona Clinic Liver Cancer
CCC	Cholangiocarcinoma
CT	Computed tomography
DAB	3,3'-Diaminobenzidine
e.g.	For example
EASL	European Association for the Study of the Liver
ECOG	Eastern Cooperative Oncology Group
FFPE	Formalin-fixed, paraffin-embedded
FNH	Focal nodular hyperplasia
GCSF	Granulocyte colony-stimulating factor
GS	Glutamine synthetase
H-HCA	HNF1A-inactivated hepatocellular adenoma
H&E	Hematoxylin and eosin
HBV	Hepatitis B virus
HCA	Hepatocellular adenoma
HCC	Hepatocellular carcinoma
HCV	Hepatitis C virus
HGDN	High-grade dysplastic nodule
HNF1A	Hepatocyte nuclear factor 1A
HRP	Horseradish Peroxidase
I-HCA	Inflammatory hepatocellular adenoma
i.e.	Id est
IHB	Intracellular hyaline body
INR	International normalized ratio
K8/18	Keratins 8/18
LCC	Large cell change

LFABP	Liver fatty acid-binding protein
LGDN	Low-grade dysplastic nodule
MDB	Mallory-Denk body
MELD	Model for end-stage liver disease
MRI	Magnetic resonance imaging
NAFLD	Non-alcoholic fatty liver disease
NASH	Non-alcoholic steatohepatitis
NOS	Not otherwise specified
PBS	Phosphate-buffered saline
RN	Regenerative nodule
SCC	Small cell change

Index of Figures

Index of Tables

1. Introduction

1.1. Structure and function of the liver

1.1.1. Gross anatomy of the liver

The liver is the largest gland in the human body. It is divided into four lobes by fibrous septa that originate from the Glisson's capsule. (1) The surface areas of the liver include the diaphragmatic surface, facing the diaphragm and a visceral surface, which is contacting the gallbladder, lesser omentum, colon, duodenum, right kidney, right adrenal gland, stomach and esophagus. (1, 2) On the diaphragmatic surface the left and right triangular ligament surrounds an area that is not covered by peritoneum, which is called "area nuda", while the falciform ligament separates the left from the right lobe. On the visceral surface quadrate and caudate lobes are present. These small lobes are framed by sulci, fossae and fissures forming the shape of the letter "H" with the porta hepatis as the center. (1) Moreover the liver can be divided by Couinaud's classification into eight segments. This classification relying on portal supply is important with regard to resections. (3)

1.1.2. Microscopic anatomy of the liver

The most two common ways to describe the microscopic anatomy of the liver are the so-called lobular and the acinar concept. Central structures of the hexagonal lobules are central veins while portal tracts can be found at the corners. (4, 5) In between there are 1 to 2 cells thick layers of hepatocytes separated by sinusoids. Both structures converge radially at the central vein. (4, 6, 7) For efficient exchange of molecules between blood and hepatocytes the sinusoids are lined by a specialized fenestrated endothelium. (8) Hepatocytes have a polygonal shape with eosinophilic cytoplasm and a round to oval nucleus. (4) Each single hepatocyte has 3 surfaces: a basolateral facing the sinusoid for substance exchange, a canalicular facing and forming the biliary canaliculus for secretion of the bile and a lateral attaching hepatocytes to each other with specialized junctions, tight junctions and gap junctions. (4, 8) The portal tracts contain the so-called Glisson's triad consisting of interlobular veins (i.e. branches of the portal vein) and arteries (i.e. branches of the hepatic artery) as well as the interlobular

bile duct which is connected to the canalicular part of the biliary system via the connecting ducts (canals of Hering). (4, 7, 8) Other cell types of the liver include the sinusoidal lining cells, the phagocytotic Kupffer cells and lymphocytes. (4) The space of Disse, located between hepatocytes and endothelial cells, contains Ito (stellate) cells and matrix components. Ito cells are important for storage of vitamin A and lipids and can transform into myofibroblasts in response to damage. (4, 6)

The acinus concept is based on portal tracts in the center and central veins at the periphery. In this concept, 3 zones (zones of Rappaport) according to decreasing oxygen saturation of the sinusoidal blood can be distinguished with zone 1 hepatocytes abiding the portal tract which are in contact with blood of higher oxygenation and zones 2 and 3 with lower and lowest oxygenation, respectively. Zone 3 surrounds the central vein. (4, 6) Normal liver histology is shown in Figure 1.

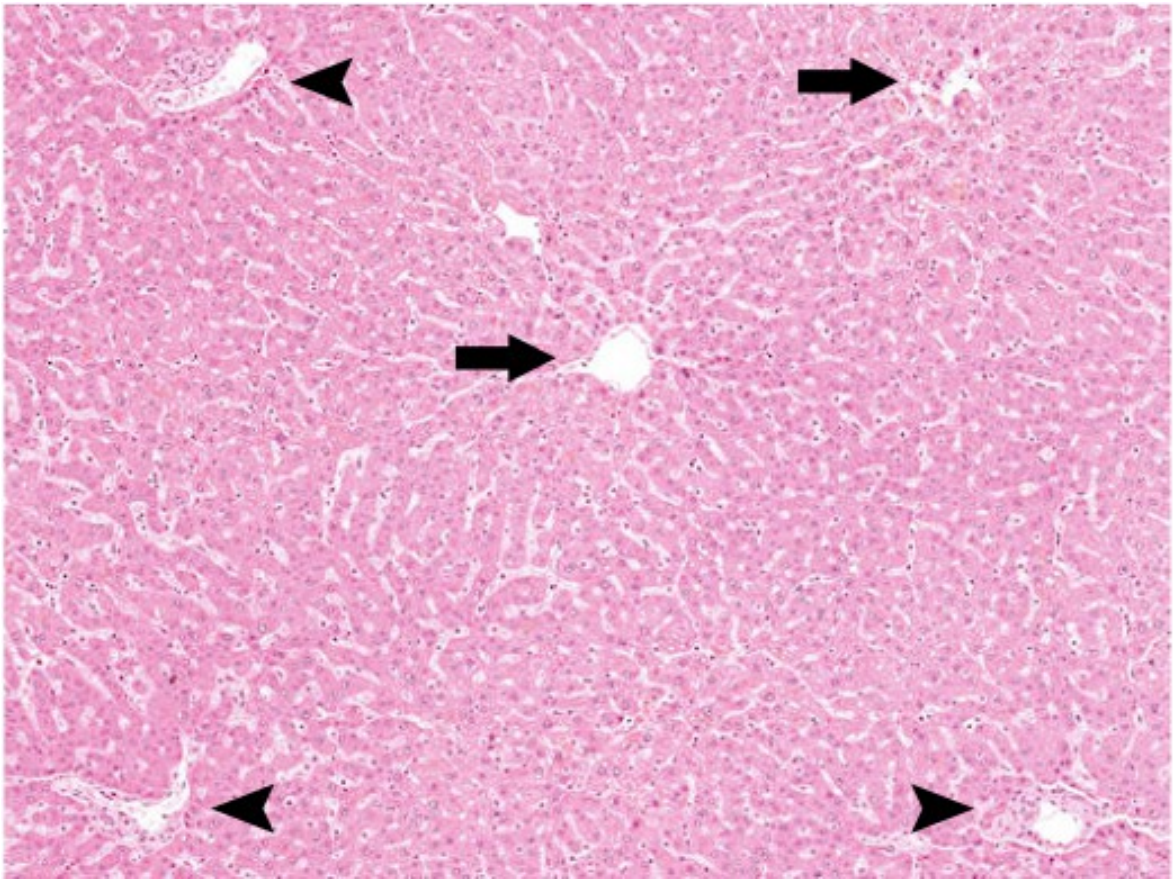

Figure 1: Normal architecture of a lobule with portal tracts (arrowheads) at the periphery and central veins (arrows) in the center. Modified after: (9)

1.1.3. Hepatic circulation

The liver receives mostly venous blood via the portal vein from the gastrointestinal tract, pancreas and spleen. Contributors to the portal vein are the inferior and superior mesenteric as well as the splenic vein. (3, 7) The hepatic artery contributes only a smaller proportion of blood. Both vessels enter the liver via the porta hepatis while the common bile duct is leaving the liver at this location. The sinusoids receive blood from both, the portal vein and the hepatic artery and are located between afferent and efferent terminal branches. The hepatic veins originating from the central veins of the lobules collect venous blood to the inferior vena cava. (8)

1.1.4. Function of the liver

As the central metabolic organ of the body the liver is involved in a variety of essential metabolic functions and plays an important role in the metabolism of biomolecules (lipids, proteins and carbohydrates) which are taken up from the nutrient-rich venous blood of the portal vein (1, 6, 7). Functions of the liver include synthesis of glycogen, serum proteins, coagulation factors, lipids and lipoproteins. (8, 10) But also storage and release of nutrients take place in the liver. (10) Additionally, the liver is essential for detoxification of both, endogenous and exogenous substances. (1) Furthermore, the liver is important for elimination of metabolites and of bilirubin. (8, 10) Notably, the liver can act as both, an exocrine and endocrine gland by releasing products either via bile secretion or directly into the blood, respectively. (1, 10)

1.2. Liver cirrhosis

Liver cirrhosis is the final stage of severe inflammatory and necrotizing liver damage by several chronic liver diseases. The production of collagen in response to liver injury leads to destruction of the lobular architecture by fibrous septa. Cirrhosis is morphologically defined by parenchymal nodules which are surrounded by fibrous septa. (6, 11, 12)

1.2.1. Etiology

Cirrhosis can arise as a consequence of many different injuries shown in Figure 2. Most common causes include alcohol (alcoholic liver disease, ALD), chronic infection with hepatitis B virus (HBV) or hepatitis C virus (HCV; chronic hepatitis B and/or C, respectively) and the metabolic syndrome (non-alcoholic fatty liver disease, NAFLD). (13, 14)

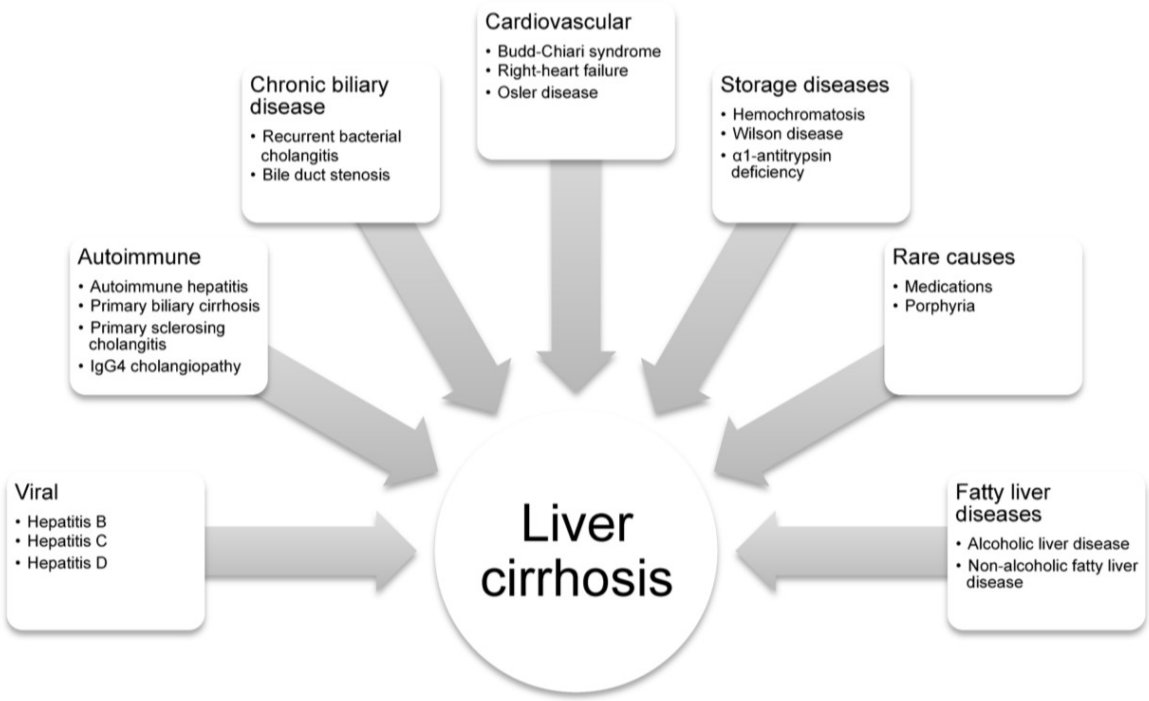

IgG4: Immunoglobulin G4

Figure 2: Causes of liver cirrhosis. Modified after: (11)

1.2.2. Pathogenesis of liver fibrosis and cirrhosis

Different types of parenchymal and mesenchymal cells are involved in the pathogenesis and progression of liver fibrosis. (14) Fibrogenesis is a multi-step process. As a consequence of liver injury with cytolysis, apoptosis or necrosis lysosomal enzymes and extracellular matrix cytokines are released from hepatocytes. (15, 16) This causes infiltration of the liver with inflammatory cells and activation of Kupffer cells. The Kupffer cells are organ specific macrophages which via the production and release of a multitude of factors aggravate liver injury and promote fibrogenesis. (5, 14, 15) Growth factors and cytokines released from

Kupffer cells induce proliferation of fibroblasts and the transition of Ito (stellate) cells from a quiescent to activated state. (14, 15) Additionally, monocytes transform into macrophages. (15) Thereby a collagen-rich extracellular matrix is produced and deposited in the space of Disse. (15, 16) The defenestration and capillarization of the sinusoidal endothelium leads to an impaired exchange capability between molecules of the blood and the liver cells. (14, 15) Furthermore, the fibrosis-associated destruction of the lobular architecture also leads to increased vascular resistance resulting in an increased blood pressure in the portal vein (portal hypertension). (6, 15, 16)

1.2.3. Macroscopic aspects of liver cirrhosis

Based on the size of the parenchymal nodules cirrhosis can be divided into macronodular (> 3 mm) and micronodular (≤ 3 mm) types. Sometimes both forms are combined (Table 1, Figure 3, Figure 4). (6, 10)

Table 1: Etiology, morphology and frequency of cirrhosis. (6)

Etiology	Predominant morphological type	Frequency (%)
Alcohol	Micronodular	60-70
Hepatitis	Macronodular, combined	10-15
Biliary (primary, secondary)	Micronodular	5-10
Hemochromatosis	Macronodular, micronodular, combined	5
Metabolic disorders	Macronodular, micronodular, combined	< 1
Toxins	Macronodular, combined	< 1
Idiopathic	Macronodular, micronodular, combined	10-20

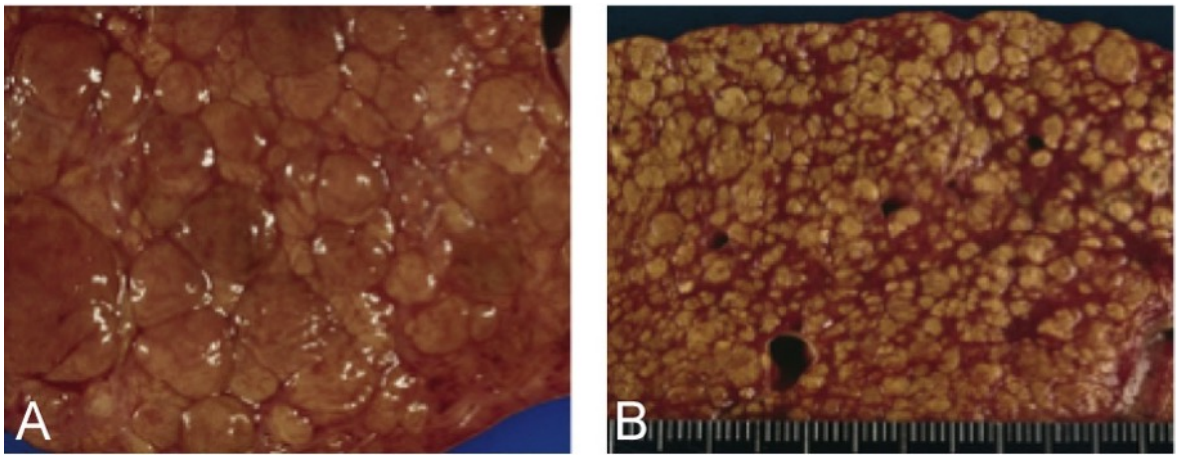

Figure 3: Macroscopic aspects of liver cirrhosis. (A) Macronodular cirrhosis showing nodules with > 3 mm in diameter separated by fibrous septa. (B) Micronodular cirrhosis composed of minute nodules measuring ≤ 3 mm. (10)

1.2.4. Histopathological aspects of liver cirrhosis

On hematoxylin and eosin (H&E) histology, macronodular cirrhosis is characterized by presence of irregular regenerative nodules surrounded by broad irregular fibrous septa. Portal tracts and efferent veins may be found. Micronodular cirrhosis shows regular regenerative nodules surrounded by thin fibrous septa, which may contain mononuclear cells and proliferated bile ductules. Central veins are absent. (6, 17) Furthermore, signs of parenchymal destruction such as necrosis and infiltration by inflammatory cells may be identified, depending on the type of liver injury. (6)

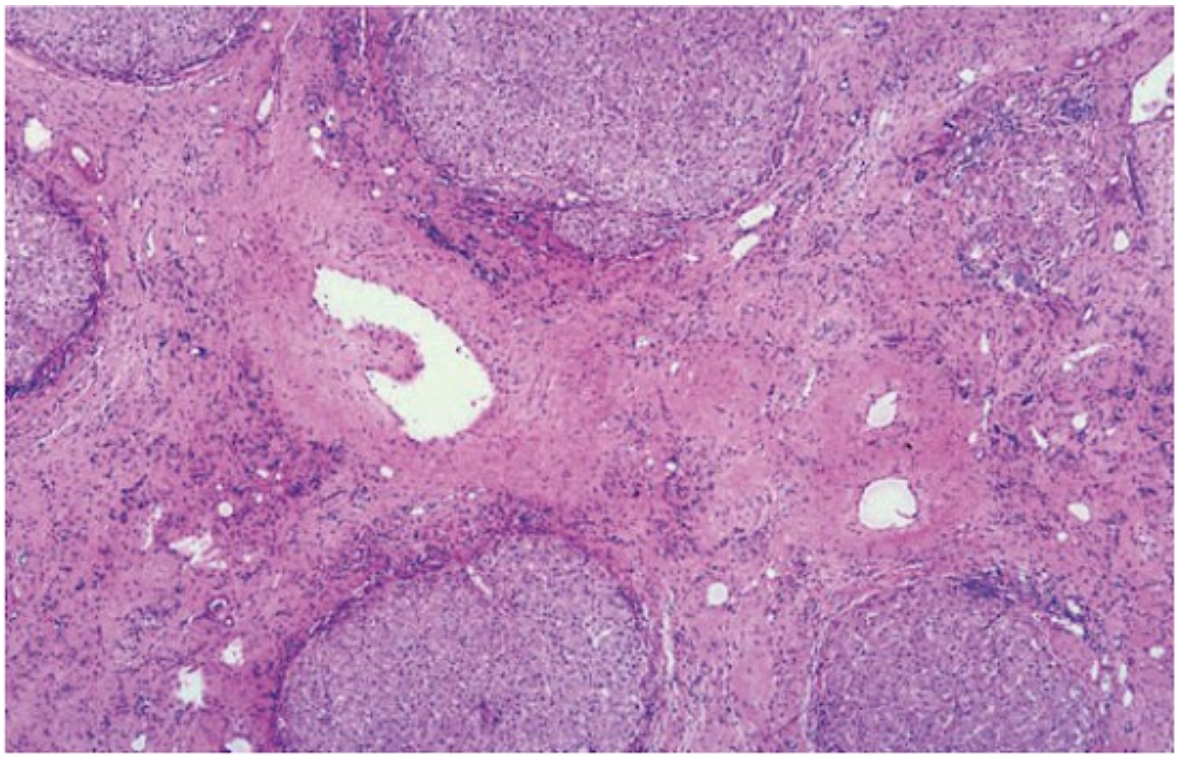

Figure 4: Histopathological features of cirrhosis. Parenchymal nodules are separated by areas of fibrosis and contain some dilated vessels. (18)

1.2.5. Clinical presentation and management of patients with cirrhosis

Liver cirrhosis often remains asymptomatic until decompensation due to progression of liver injury and fibrogenesis occurs. (19, 20) Patients with decompensated cirrhosis are characterized by ascites, jaundice, esophageal varices which can be complicated by life-threatening bleeding events. Esophageal varices are a consequence of portal hypertension. Other complications of cirrhosis

include splenomegaly and hepatic encephalopathy. Due to impaired immune defense bacterial and fungal infections can occur more frequently than in patients with non-cirrhotic liver disease. (19, 21)

Importantly, cirrhosis paves the way for the development of hepatocellular carcinoma (HCC). (19, 22, 23) HCC arises in 80 to 90% of cases in cirrhotic livers and only rarely in earlier stages of fibrosis or in normal liver. (24-26)

Prognostic scores based on non-invasive clinical and biochemical parameters have been developed to guide treatment decision of patients with cirrhosis. The most widely used are the Child-Turcotte-Pugh score (Table 2) and Model for End-stage Liver Disease (MELD) score. (27)

Table 2: Parameters contributing to the Child-Turcotte-Pugh score. (22)

Parameter	**1 Point**	**2 Points**	**3 Points**	
Albumin (g/dl)	> 3.5	2.8 – 3.5	< 2.8	Addition: Child A: 5 – 6 Child B: 7 – 9 Child C: 10 – 15
Bilirubin (mg/dl)	< 2.0	2.0 – 3.0	< 3.0	
Quick (%)	> 70	40 – 70	< 40	
Ascites (ultrasound)	0	Mild	Moderate	
Encephalopathy	0	I – II	III – IV	

The 1-year survival rates for Child-Turcotte-Pugh score classes A, B and C are 95%, 80% and 44%, respectively. (28) Parameters contributing to the MELD score include serum creatinine and bilirubin concentrations as well as the international normalized ratio (INR). The MELD score is calculated by a mathematical formula. (23) Values are ranging from 6 to 40. The cut-off for considering the listing of patients for liver transplantation was set to a MELD score ≥ 15. (28)

Therapeutic approaches for patients with liver cirrhosis include treatment of underlying liver diseases which is essential to impair and ideally stop disease progression. (22, 29) In addition, management of potentially life-threatening complications of cirrhosis, variceal bleeding, ascites, hepatic encephalopathy,

renal failure or infection contributes to better quality of life and patient survival. (19, 22) General measures depending on the etiology of chronic liver disease such as weight loss, abstinence from alcohol and smoking as well as dietary measures (adequate supply of calories, proteins and vitamins) are also important to reduce risk of complications and mortality. (22, 29)

1.3. Hepatocellular carcinoma

1.3.1. Epidemiology

HCC is among the most common types of cancer and the second most common cause of cancer-related death worldwide. (30) The incidence and etiology of HCC vary depending on geographical area. (25, 31) Less developed countries have the highest rates with more than 80% of worldwide reported cases. (31) Besides China and Japan high incidence is observed in sub-Saharan Africa due to endemic chronic HBV infection and aflatoxin intoxication whereas in Italy, Spain and Greece moderately high incidence rates are associated with chronic HCV infection and/or metabolic syndrome and/or alcohol-related fatty liver disease. North and South America, South-Central Asia, Northern Europe, Australia and New Zealand show lowest burden of HCC. (30-33)

1.3.2. Risk factors

Most important risk factors for the development of HCC are chronic infection with HBV and/or HCV, the metabolic syndrome and/or alcohol abuse. (24, 25, 31) Also tobacco-smoking, high dietary ingestion of aflatoxin B1 and metabolic disorders like hereditary hemochromatosis, Mb. Wilson or α1-antitrypsin deficiency have been identified as risk factors. (24, 31) Other risk factors are male sex which may at least be partially attributable to life style habits such as alcohol and nicotine consumption. Other risk factors more prevalent in men than in women include acquired viral hepatitis and high body mass index. In addition, testosterone has also been linked to the higher incidence of HCC in males. (24)

1.3.3. Macroscopy

The macroscopic types of HCC include nodular, diffuse and massive subtypes. (31) Most commonly HCC are (multi-)nodular lesions. Diffuse (or cirrhotomimetic) HCC are characterized by presence of numerous small nodules occupying a lobe or wide parts of the whole liver. (31, 34) The massive subtype is defined by a large poorly circumscribed mass that may have smaller satellite nodules. (31, 34, 35) Due to the low stroma content most HCC have a soft consistence compared to surrounding non-neoplastic, often cirrhotic liver. (36) The colour of cut surface can vary between yellow, brown and green depending on fat and bile content. (10, 31, 37) Particularly, in larger tumors necrotic and hemorrhagic areas may be seen (Figure 5). (5, 38)

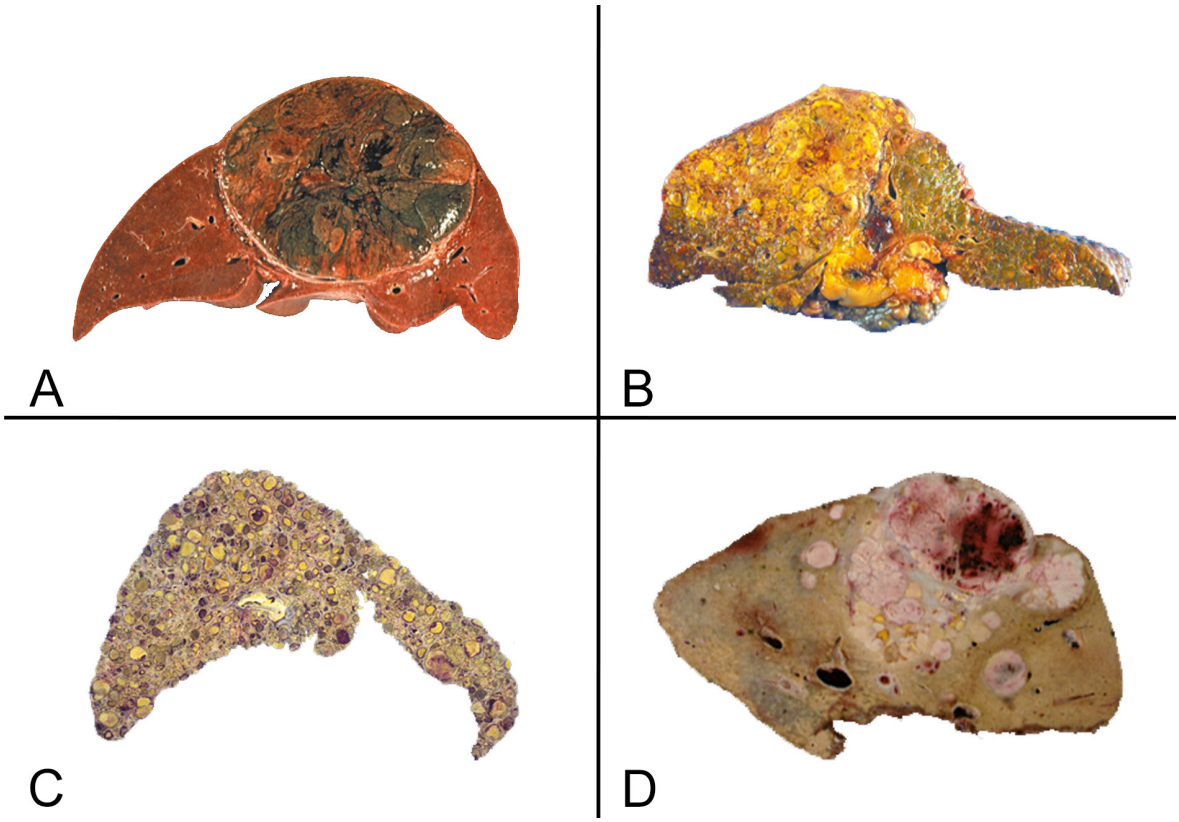

Figure 5: Macroscopic aspects of hepatocellular carcinoma. (A) Nodular subtype. A nodular single tumor with a thin fibrous pseudocapsule and a yellow-brown and green cut surface. (B) Massive subtype. Tumor mass replacing most of the lobe. (C) Diffuse subtype. Multiple small tumor nodules resembling cirrhosis. (D) Massive subtype with hemorrhage and satellite nodules. Modified after: (31)

1.3.4. Histopathology

Most common growth patterns of HCC include trabecular, pseudoglandular/acinar or solid/compact pattern (Figure 6). (34, 39) The trabecular pattern is composed of several layers of tumor cells covered by a layer of non-fenestrated endothelium. (34, 35, 40) The polygonal tumor cells are typically smaller and show a more basophilic cytoplasm than non-neoplastic hepatocytes. (6, 35, 39) Nuclear atypia varies according to differentiation grade. (39) Multinucleation and giant tumor cells may be observed. (6) The sinusoidal equivalents between the tumor trabeculae are supported by significantly decreased reticulin fiber network. The number of Kupffer cells may be decreased in well-differentiated and missing in poorly differentiated HCC. (6, 35, 39, 41) The pseudoglandular growth pattern is typically combined with trabecular growth pattern. It features gland-like structures formed by tumor cells as a result of canalicular dilatation between neoplastic cells. Pseudoglands may contain bile or proteinaceous fluids. (31) Poorly differentiated tumors show a solid growth pattern which is characterized by compressed thick trabeculae and thin sinusoid vascular spaces. (31, 35) Owing to the numerous sinusoidal equivalents and unpaired arterial branches HCC are highly vascularized. (34, 42) Vascular invasion by neoplastic cells is a common feature. (34) Portal tracts are absent in HCC. (31) Bile production is often seen in well-differentiated HCC. (34) Poorly differentiated HCC show high nuclear to cytoplasmic ratio, sparse basophilic cytoplasm and high degree of nuclear pleomorphism. (39)

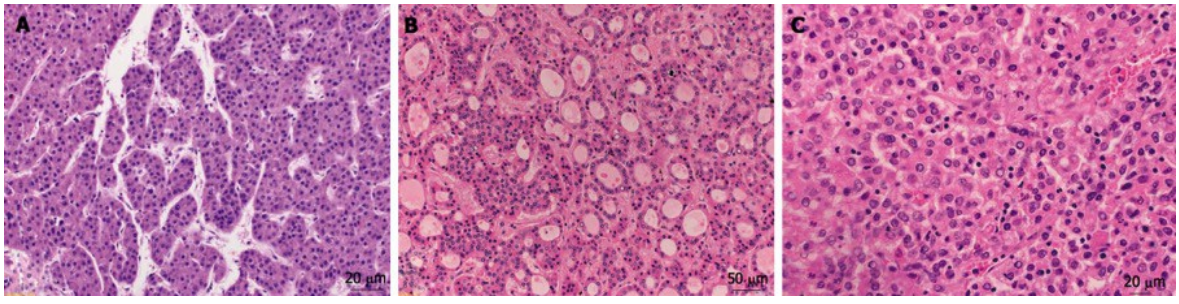

Figure 6: Growth patterns of hepatocellular carcinoma. (A) Trabecular growth pattern. (B) Pseudoglandular growth pattern. (C) Solid growth pattern. (39)

Several histochemical and immunohistochemical markers have been described that can be used for the characterization of HCC and for differential diagnosis with other tumors in the liver eventually resembling HCC and/or differentiation of non-malignant preneoplastic precursors (see below) from HCC (Table 3). (39, 40)

Table 3: Immunohistochemical features of hepatocellular carcinoma. Modified after: (39, 40)

Histochemical and immunohistochemical stains	Feature in HCC cells
Reticulin	Loss of reticulin
CD34	Labels endothelial cells of sinusoidal equivalents but not normal sinusoids of non-neoplastic liver
Glypican 3, HepPar1	Cytoplasmic staining
CD10, pCEA	Canalicular markers
Arginase-1	Cytoplasmic and nuclear staining

HCC: Hepatocellular carcinoma

Differentiation grade can be described by the modified Edmondson-Steiner-grading system. This system is among the most widely used systems for HCC grading (Table 4). (35, 39)

Table 4: Modified Edmondson-Steiner grading system. (39)

Grade	Criteria
1	Abundant cytoplasm, minimal nuclear atypia
2	Mild nuclear atypia with prominent nucleoli, hyperchromasia, nuclear irregularity
3	Moderate nuclear atypia with greater hyperchromasia and nuclear irregularity
4	Marked nuclear pleomorphism, marked hyperchromasia, anaplastic giant cells

1.3.5. Hepatocellular carcinoma variants

Several variants of HCC have been described (39):

- Biphenotypic HCC
- Cirrhotomimetic HCC
- Clear cell carcinoma
- Granulocyte colony-stimulating factor (GCSF) producing HCC
- Hepatic stem cell carcinoma/hepatic progenitor cell carcinoma
- Lymphocyte-rich HCC
- Sarcomatoid HCC
- Scirrhous HCC
- Steatohepatitic HCC
- Fibrolamellar HCC

1.3.6. Management of HCC

Patients with cirrhosis should be included in screening programs for early detection of HCC. Current guidelines recommend ultrasonographic liver screening at an interval of six months. In some patients with HCC alpha-fetoprotein (AFP) levels in serum can be used as a tumor marker for monitoring of treatment and during follow-up. (22, 29, 43) The Barcelona Clinic Liver Cancer (BCLC) staging classification is recommended by the American Association for the Study of Liver Diseases (AASLD) and European Association for the Study of the Liver (EASL) for the management of patients with HCC. (44-46) According to the extension of the tumor, liver function (represented by the Child-Turcotte-Pugh score), performance status (Eastern Cooperative Oncology Group, ECOG) and cancer related symptoms patients with HCC are subsequently assigned to five groups (0, A-D). (46) Adequate therapies are assigned to each of these groups. Curative treatment is possible in Stage 0 and A. Moreover, the groups differ with regard to survival rates (Figure 7). Patients at (very) early stage show an overall survival of more than 60 months whereas overall survival is less than 3 months at the terminal stage. (44)

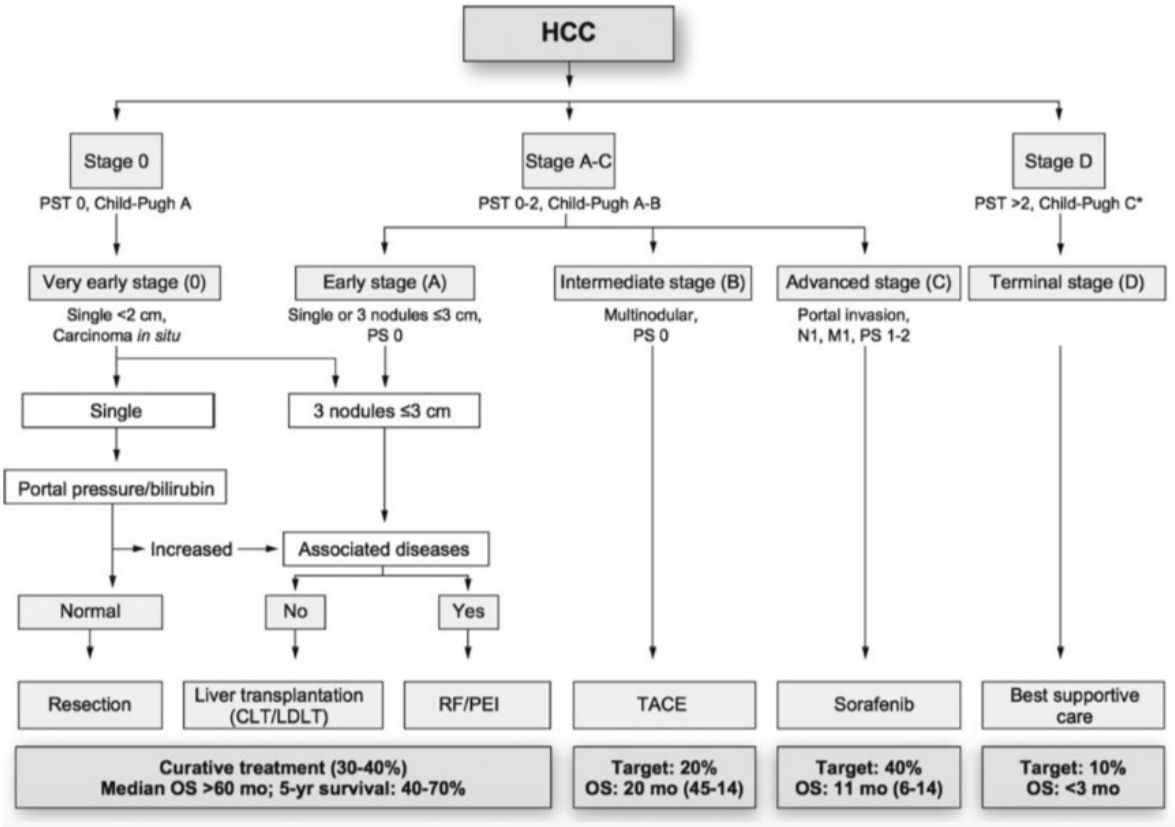

CLT: Cadaveric liver transplantation; LDLT: Living donor liver transplantation; OS: Overall survival; PS: Performance status; PST: Performance status test; RF/PEI: Radiofrequency ablation/percutaneous ethanol injection; TACE: Transcatheter arterial chemoembolization

Figure 7: Barcelona Clinic Liver Cancer (BCLC) staging system facilitates stratification of patients according to their disease stage, liver function (Child-Turcotte-Pugh score), PST and cancer-associated symptoms in order to provide adequate therapies. While patients at (very) early stage fit for curative treatment and have OS rates of > 60 months patients at terminal stage show OS of < 3 months. (44)

1.4. Cytoplasmic hyaline inclusions

HCC cells may contain cytoplasmic inclusions including Mallory-Denk bodies (MDB), pale bodies, intracellular hyaline bodies (IHB) and/or lipid droplets. (31, 47)

1.4.1. Degradative Pathways and formation of hyaline inclusions

Autophagy is a lysosomal process of degradation. It is involved in degradation of defective organelles as well as misfolded or aggregated proteins. (48-50) Impaired autophagy can be found in several diseases like HCC and is linked to accumulation of misfolded protein aggregates. (50) The second, predominant way for degrading proteins is the ubiquitin-proteasome system and is also able to contribute to formation of inclusions. (51, 52) P62 is a signaling molecule and an autophagy receptor protein. (53) It can be used as flux index because it accumulates in case of impaired autophagy. (52, 54) P62 has the ability to bind ubiquitinated cargo and deliver it to the autophagic machinery as well as to the proteasome for degradation. (52, 55) In case of impaired autophagy and/or overwhelmed ubiquitin-proteasome system MDB and IHB may be formed as a consequence of accumulation of substrates. (47)

1.4.2. Mallory-Denk bodies

Mallory-Denk bodies are intermediate filament-related, intracytoplasmic aggregates in hepatocytes consisting mainly of phosphorylated cytoskeletal keratins 8 and 18 (K8/18) proteins, p62 and ubiquitin. (51) MDB can be found in several chronic liver diseases such as ALD, NAFLD and HCC. (17, 51) They mainly result from chronic hepatocellular injury due to oxidative stress and eventually other cellular stresses. (47, 51) Mechanisms leading to formation as well as accumulation of MDB include oxidative stress-associated overexpression of K8 compared to K18, hyperphosphorylation, misfolding, crosslinking of K8/18, association with p62 and ubiquitin and impaired degradation of the resulting protein aggregates by proteasomal overload. (47, 51, 56) Notably, MDB in benign and malignant disease show similar composition. (47, 51) On H&E microscopy, MDB are irregularly shaped hyaline inclusions which may also take the shape of strands or garlands. (47, 51) Although MDB typically are found close to the

nucleus they may also be detected at the cell periphery. (51) According to the underlying liver disease occurrence of MDB in hepatocytes differs with respect to lobular zonation: While MDB occurring in ALD or NAFLD affect perivenular mostly ballooned hepatocytes they are usually found in periportal hepatocytes in amiodarone toxicity. (57-59) H&E morphology is illustrated in Figure 8.

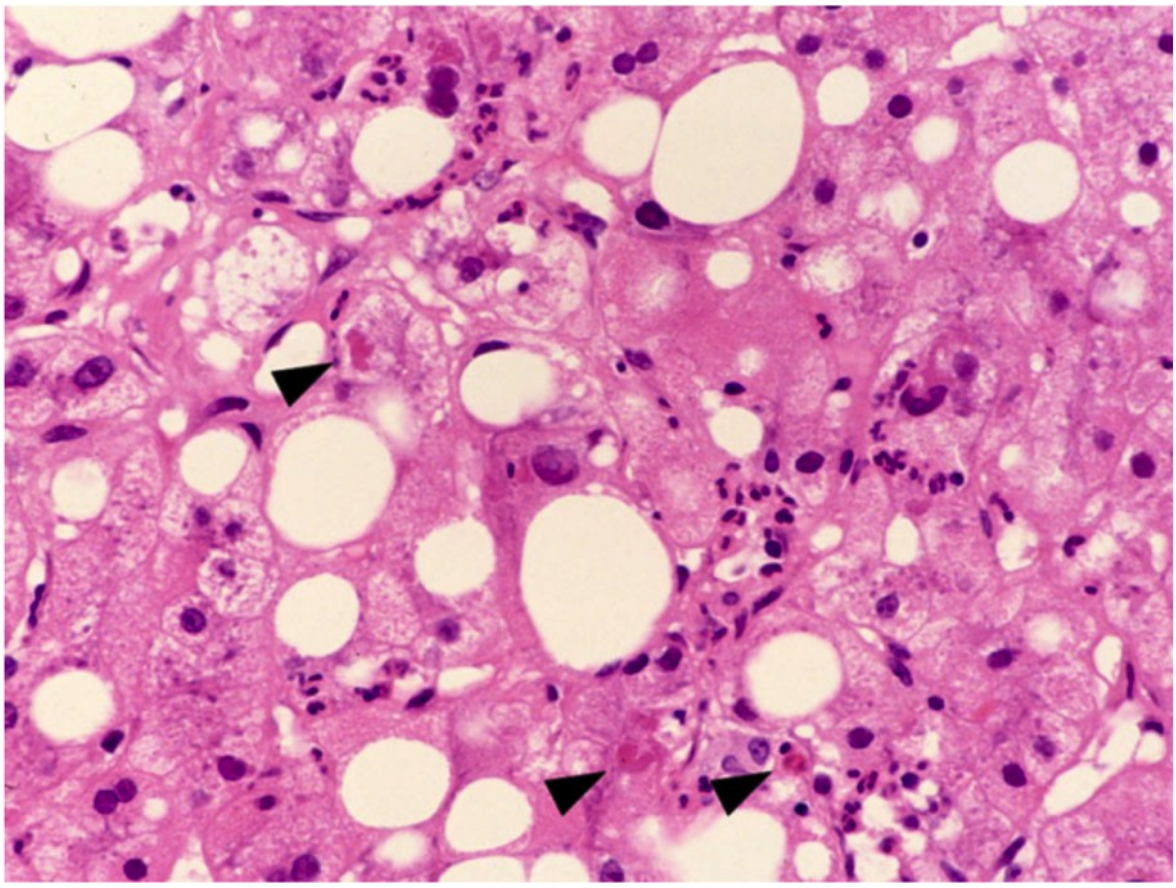

Figure 8: Ballooned hepatocytes with Mallory-Denk bodies (MDB) in a case of alcoholic steatohepatitis. Enlarged hepatocytes with rounded cell shape and lightly stained cytoplasm contain eosinophilic hyaline irregularly shaped inclusions, MDB (indicated by arrowheads). (58)

1.4.3. Intracellular hyaline bodies

In contrast to MDB, intracellular hyaline bodies are composed of p62 and ubiquitin or p62 only. (51, 60) This type of inclusion can be found in HCC, in cholangiocarcinomas (CCC) and some forms of copper toxicosis. (9, 47) As illustrated in Figure 9, IHB appear as homogenous deeply eosinophilic, hyaline

and globular inclusion bodies. They often are surrounded by a clear halo. (9, 47, 51)

In HCC tumor cells MDB and IHB may coexist as separate structures or in a combined form called "hybrid" inclusions. (47, 51) Figure 10 shows MDB and IHB on H&E- as well as immunostains with K8/18, p62 and ubiquitin.

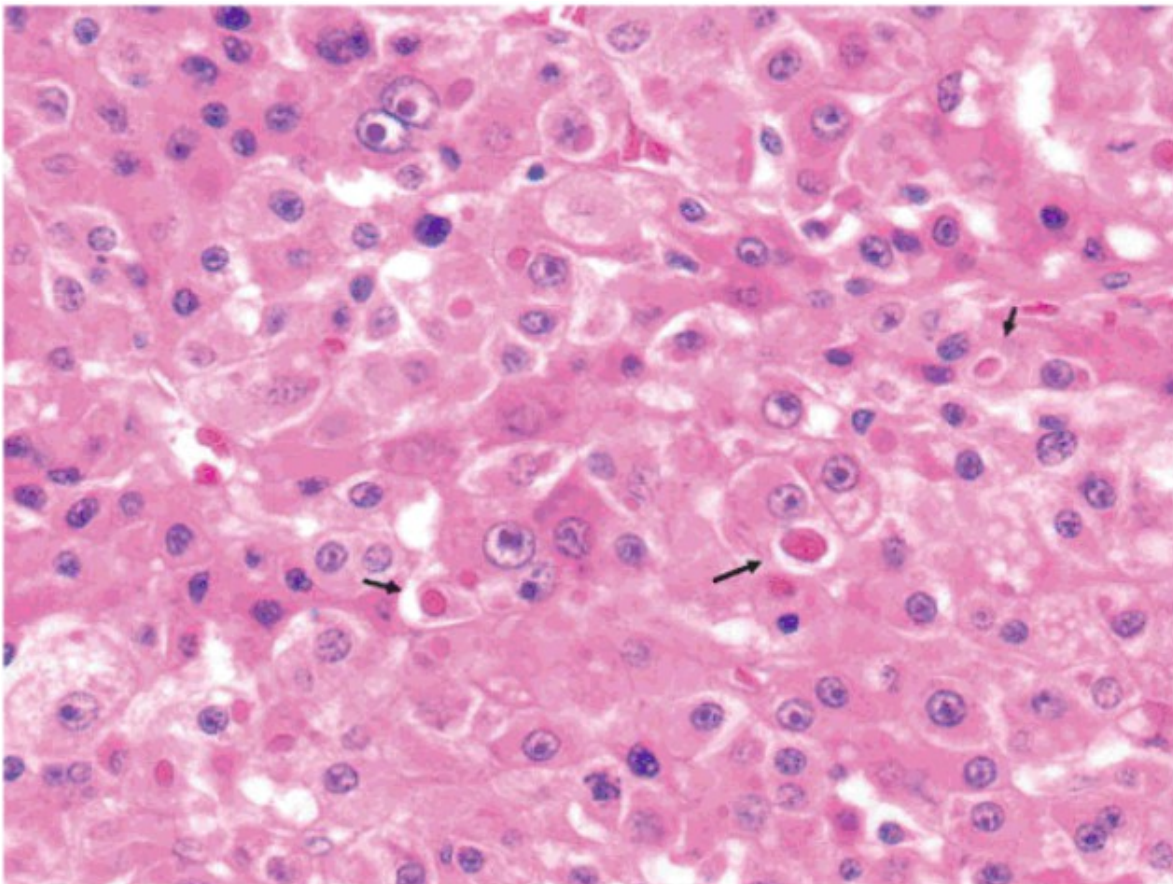

Figure 9: Intracellular hyaline bodies (arrows) in case of hepatocellular carcinoma. (61)

1.4.4. Other types of inclusions

Other types of inclusions include ground glass inclusions, megamitochondria, α1-antitrypsin globules and fibrinogen inclusions (fibrinogen storage bodies and pale bodies, respectively). These differ from MDB and IHB with respect to morphology and composition as demonstrable by immunohistochemistry (Table 5). (9, 51, 62)

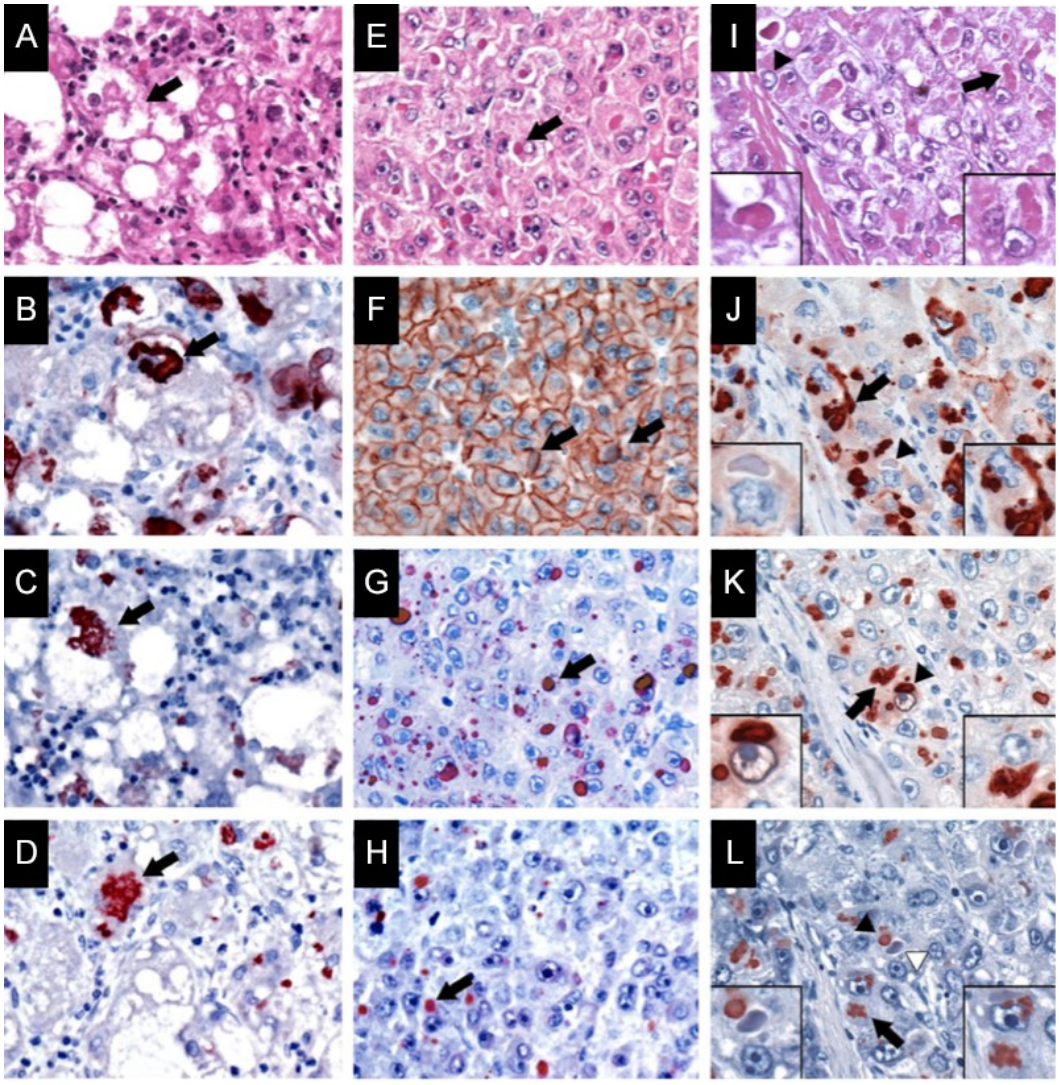

Figure 10: Keratins 8/18 (K8/18), p62 and ubiquitin expression in hepatocellular carcinoma (HCC) cells containing intracytoplasmic hyaline inclusions. (A-D) Tumor cells with Mallory-Denk bodies (MDB) only (arrows). (A) On hematoxylin and eosin (H&E) histology, a tumor cell exhibits steatohepatitic features and shows a large MDB. MDB show reactivity with antibodies against K8/18 (B), p62 (C) as well as ubiquitin (D). (E-H) Tumor cells with intracellular hyaline bodies (IHB) only (arrows). (E) On H&E histology, IHB are globular eosinophilic inclusions within HCC cells. IHB are stained with p62 (G) and occasionally with ubiquitin (H) but are not stained with K8/18 (F). (I-L) Tumor cells containing both, MDB (arrows; zoomed in insets) and IHB (arrowheads; zoomed in insets). (I) On H&E histology, the HCC cells show both, MDB and IHB. (J) MDB are stained with K8/18 whereas IHB are negative. (K) MDB and IHB are stained with p62. (L) MDB and some IHB are stained with ubiquitin. Some IHB do not show reactivity with antibodies against ubiquitin. Modified after: (47)

Table 5: Hepatocellular intracytoplasmic inclusions and immunohistochemical features. Modified after: (63)

Intracytoplasmic inclusion types	Reactivity on immunohistochemistry
Mallory-Denk bodies	K8/18+, p62+, ubiquitin+
Intracellular hyaline bodies	p62+, K8/18-, ubiquitin+/-
α1-antitrypsin globules	α1-antitrypsin+, p62-, K8/18-, ubiquitin-
Megamitochondria	Antibodies against mitochondria+, p62-, K8/18-, ubiquitin-
Fibrinogen storage bodies/pale bodies	Fibrinogen+, occasionally albumin+, p62-, K8/18-, ubiquitin-

+/-: Positive/negative; K8/18: Keratins 8/18

1.5. Precursor lesions of HCC in cirrhotic liver

In most cases HCC development in cirrhotic liver occurs in a multistep fashion (Figure 11). (64, 65)

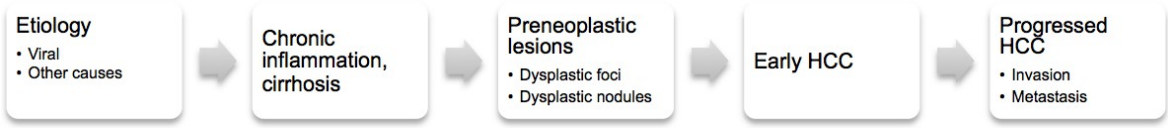

HCC: Hepatocellular carcinoma

Figure 11: Multistep scheme of hepatocarcinogenesis. Preneoplastic lesions develop in cirrhotic liver. Increasing severity of dysplasia is mirrored by accumulation of genetic alterations. Dysplastic foci and/or low-grade dysplastic nodules precede the development of high-grade dysplastic nodules and finally early and advanced types of HCC. Modified after: (64, 66)

1.5.1. Dysplastic foci

Dysplastic foci consist of atypical hepatocytes arranged in clusters. Usually these lesions measure < 1 mm in diameter and therefore can only be detected on histology. (66, 67) Dysplastic foci are mostly observed in a cirrhotic background. Two forms, small and large cell dysplastic foci (i.e. small and large cell change, respectively) defined by the size of dysplastic hepatocytes have been described (Figure 12). (67)

Small cell change (SCC). Hepatocytes are characterized by smaller size than normal hepatocytes. They show a basophilic cytoplasm, high nuclear to cytoplasmic ratio as well as nuclear hyperchromasia and pleomorphism. (65, 67, 68) Multinucleation may occur. (69) Beyond the higher proliferative activity other findings such as chromosomal alterations as well as lacking of E-cadherin expression support the precancerous nature of SCC. (67, 68) While expansile growth is considered to be associated with HCC development a diffuse pattern may rather represent regeneration. (67) Recent studies suggest that SCC may be a more advanced precancerous lesion than large cell change. (65)

Large cell change (LCC). LCC consists of enlarged hepatocytes with large hyperchromatic and polymorphic nuclei but preserved nuclear to cytoplasmic ratio. (65, 67) Also in this condition multinucleation can be a feature. In contrast to SCC, findings in areas of LCC such as a low proliferative activity and an increased apoptotic rate may imply a reactive or senescent rather than a neoplastic nature of LCC. (67) However, LCC has been described as a risk factor for malignant transformation, in particular in patients with chronic HBV infection and cirrhosis. (65, 68)

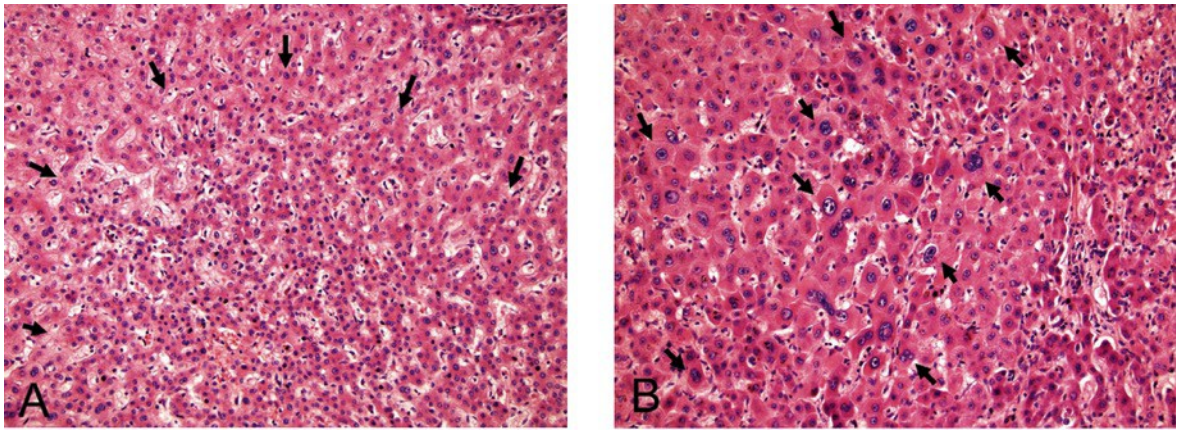

Figure 12: Liver cell dysplasia. (A) In small cell change (arrows) the atypical hepatocytes are smaller and more basophilic than surrounding normal hepatocytes and show an increased nuclear to cytoplasmic ratio. (B) Areas of large cell change (arrows) are characterized by presence of large hepatocytes with abundant cytoplasm and large hyperchromatic nuclei (arrows). Therefore the nuclear to cytoplasmic ratio is not increased. (67)

1.5.2. Dysplastic nodules

Dysplastic nodules can be divided into low- and high-grade dysplastic nodules (LGDN and HGDN, respectively). (67) They occur in cirrhotic liver and represent premalignant lesions of HCC. (67, 68) Based on nodal size, color, texture and degree of bulging at the cut surface they can be distinguished macroscopically from the regenerative nodules of the cirrhotic liver. (66, 68)

LGDN. Although LGDN sometimes occur as vaguely nodular lesions they are mostly rimmed by condensed scarring. (70, 71) The nodules are characterized by

slightly increased cellularity with a monotonous pattern but usually no appreciable cytologic atypia. (65, 67) LCC may be seen in- and outside of the LGDN and clonal changes such as clear cell change may be present. (66, 67) LGDN may show a decreased number of portal tracts and so-called unpaired arteries (i.e. arterial branches not accompanied by portal vein branches) as compared to regenerative nodules (RN) of background cirrhosis (Figure 13). (65, 67, 70)

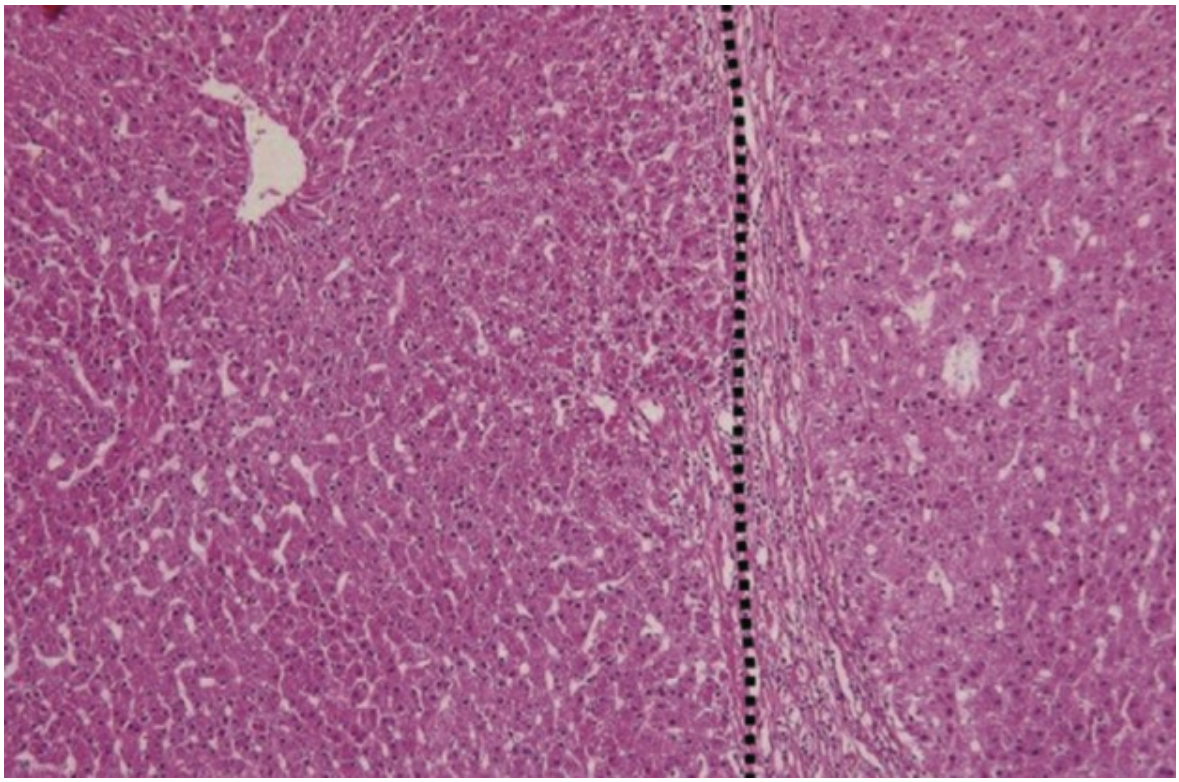

Figure 13: Histopathological features of low-grade dysplastic nodule (LGDN) in cirrhotic liver. LGDN (left side of image, separated by dotted line from background regenerative nodule (RN)) shows mildly increased cellularity. The slightly atypical hepatocytes are smaller and are more intensely stained than the RN (right of the dotted line). (66)

HGDN. This type of precancerous lesion bears a higher risk for malignant transformation than LGDN. (65) While LGDN frequently arise as distinctly nodular lesions HGDN often appear vaguely nodular. (70) In contrast to LGDN, they show at least moderate cytologic atypia. (67) They are arranged in atypical trabecular structures 1 to 2 cells wide and the cytologic atypia falls short of a diagnosis of HCC. (67, 70) Other findings in HGDN include increased cellularity, decreased

number of portal tracts and increased number of unpaired arteries (Figure 14). SCC and a nodule-in-nodule arrangement of atypical hepatocytes up to foci of frank HCC may be seen. (65, 67, 70)

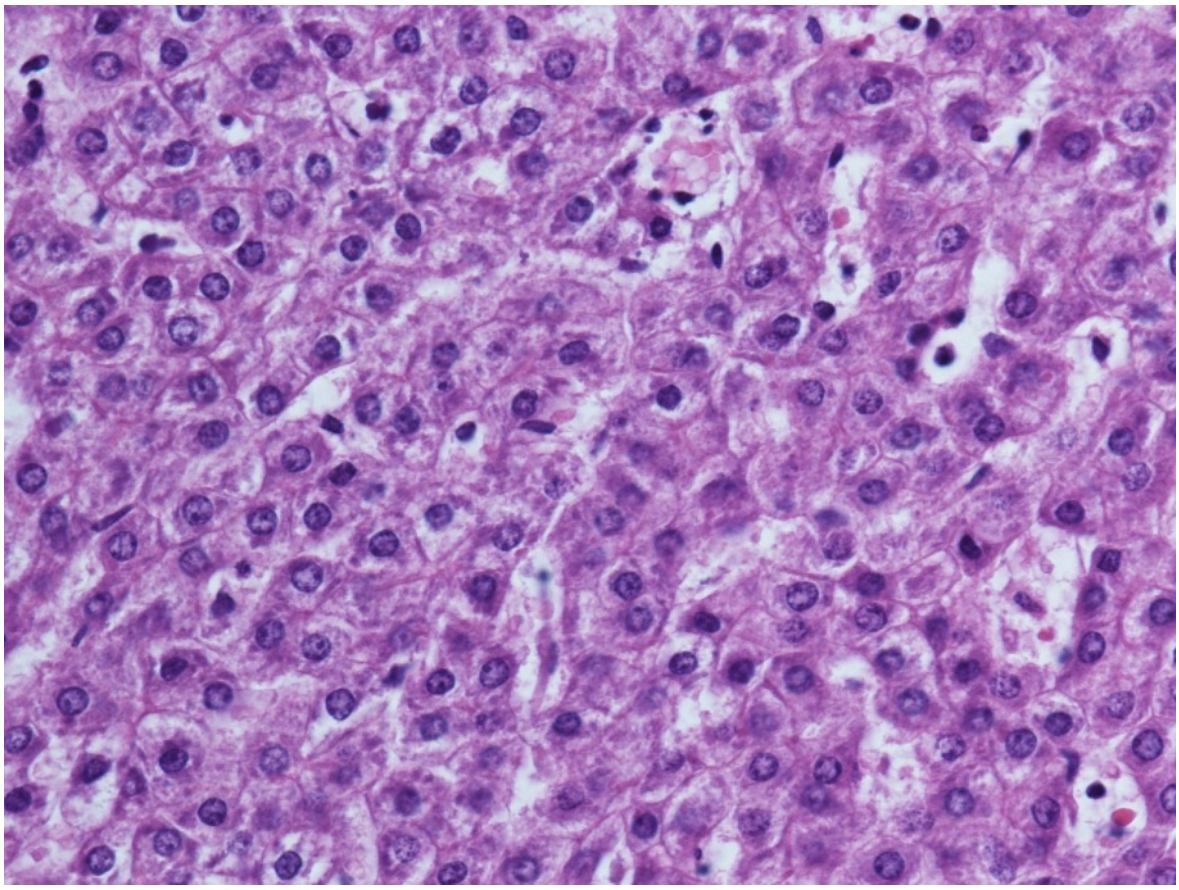

Figure 14: High-grade dysplastic nodule with increased cellularity and irregular trabecular growth pattern. (Own representation)

1.6. Precursor lesions of HCC in non-cirrhotic liver

1.6.1. Hepatocellular adenoma

Hepatocellular adenomas (HCA) are rare benign neoplasms that arise in a background of non-cirrhotic liver. (72) They occur more frequently in women than in men. (73) Risk factors for the development of HCA include oral contraceptives, androgenic steroids, diabetes mellitus, metabolic syndrome and genetic disposition. (73-76) Macroscopically, HCA is a nodular parenchymal mass composed of normal hepatocytes in trabecular arrangement and sinusoids. (6, 73) Portal tracts are absent. (6) Blood supply is via arterioles with sparse adventitial fibrous tissue. (77) HCA cells may harbor cytoplasmic inclusions like lipid droplets, pigments or glycogen. (73) MDB may be present. (78) Risk factors for malignant transformation include oral contraceptives, androgenic and anabolic steroids, male sex, glycogen storage disease and β-catenin activation. (74) HCA can be divided into several subtypes (Table 6). (74)

Table 6: Frequency, risk of malignant transformation, antigenic properties and histopathological features of hepatocellular adenoma subtypes. Modified after: (39, 73, 74)

HCA type	HNF1A-inactivated	Inflammatory	β-catenin activated	Unclassified
Frequency (%)	30-50	35	10-15	5-10
Malignant transformation	Rarely	No	Yes	No
Markers	Liver fatty acid-binding protein-	Serum amyloid A+, C-reactive protein+	β-catenin+, glutamine synthetase+	None
Microscopy	Diffuse steatosis	Ductular reaction, dilated and congested sinusoids, large unpaired arteries, inflammatory infiltrates	Cholestasis, cytologic and architectural atypia	No features of other subtypes

+/-: Positive/negative; HCA: Hepatocellular adenoma; HNF1A: Hepatocyte nuclear factor 1A

1.6.2. Focal nodular hyperplasia

Focal nodular hyperplasia (FNH) is a frequent benign reactive tumor and accounts for 8% of all liver neoplasms. (39, 73) Although FNH arise in the majority of cases in young to middle-aged women it is hormonally independent and not affected by oral contraception intake and pregnancy. (39, 73) In about 80% of cases FNH are single lesions but multiple forms have also been described. (73) As suggested by some authors, FNH may very rarely undergo malignant transformation. (79) Macroscopically, FNH are well demarcated lesions in a non-fibrotic/cirrhotic liver. (39, 80) They are composed of parenchymal nodules surrounded by fibrous septa resembling cirrhosis. (39, 73) In the center, they show a fibrous scar with septa radiating at the periphery of the tumor. (6, 73) On microscopy, the parenchymal nodules are composed of normal hepatocytes in trabecular arrangement and regular sinusoids. (81) Within the septa proliferated bile ductules (ductular reaction) can often been found. (6) Typically, regular bile ducts are absent. Prominent vessels with abnormally thickened walls are found within the septa. They are most prominent in the central scar. Hepatocytes of FNH may contain lipid droplets, bile pigment or copper deposits. Hepatocellular ballooning and MDB may be seen. On immunohistochemistry, FNH are characterized by irregularly shaped areas of hepatocytes which stain with antibodies against glutamine synthetase (map-like staining pattern; Figure 15). (39, 73) This staining pattern is helpful in the differential diagnosis with HCA which does not show this immunohistochemical feature. (39)

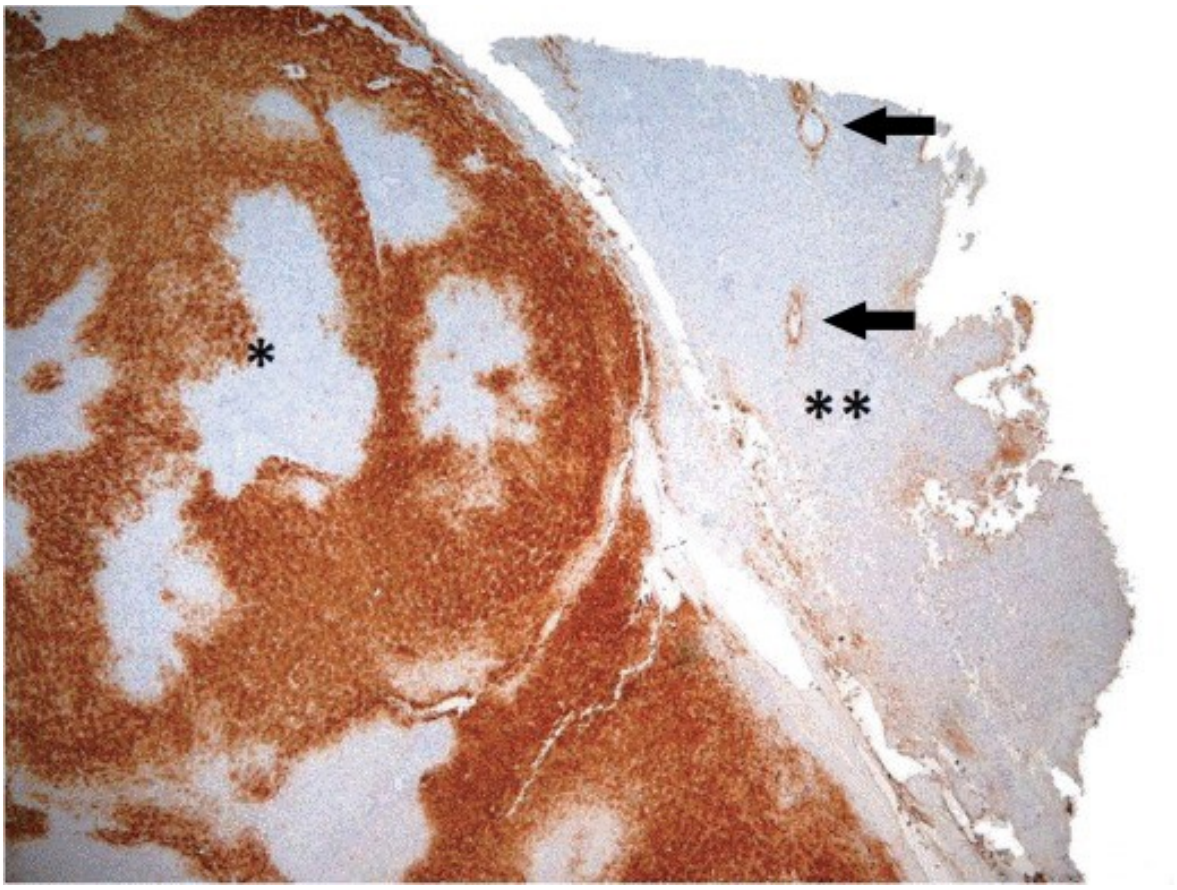

Figure 15: Map-like staining pattern of glutamine synthetase (GS) in FNH (*) as compared to non-tumoral liver (**) where GS-antibodies stain only perivenular hepatocytes (arrows). Modified after: (73)

2. Objectives

Intracytoplasmic hyaline inclusions of MDB type have been described in hepatocytes in settings of chronic oxidative stress, mostly in alcoholic and non-alcoholic steatohepatitis (ASH and NASH, respectively), toxic liver damage or cholestasis, in tumor cells in benign liver tumors including HCA and FNH and malignant tumors of the liver, HCC and CCC. (82) In contrast, it is not clear whether IHB can also occur in these conditions. So far IHB have only been described as features of HCC on light microscopy. They are distinct features which are easy to detect and could thus serve as inexpensive tumor markers. However, MDB and IHB inclusions of small size may be missed on H&E histology and may be detected with higher sensitivity and specifity by immunohistochemistry.

3. Hypothesis

We hypothesize that IHB are only present in HCC and are not found in hepatocytes of regenerative cirrhotic nodules or precursor lesions of HCC in cirrhotic liver, dysplastic foci, LGDN, HGDN or in non-cirrhotic liver, HCA and FNH.

4. Aims

In this study we will analyze precursors of HCC in cirrhotic and non-cirrhotic liver as well as in non-neoplastic liver cells for presence of MDB and IHB by light microscopy and immunohistochemistry and evaluate utility of these cytoplasmic inclusions as tumor markers of HCC.

5. Patients, materials and methods

5.1. Ethical considerations

The study was approved by the Ethical Review Committee of the Medical University of Graz (EK 29-159 ex 16/17).

5.2. Patients

Regenerative nodules and HCC precursor lesions were identified from a cohort of 107 consecutive patients resected or transplanted for HCC between 2006 and 2017 at the Medical University of Graz (HCC cohort). From all patients formalin-fixed and paraffin-embedded (FFPE) tumor and non-neoplastic liver tissue was available and provided by the Biobank of the Medical University of Graz. In addition, the archive of the Diagnostics and Research Institute of Pathology was searched for cases who underwent liver resection for HCA between 2006 and 2011 or FNH between 2011 and 2016.

5.3. H&E histology

HCC cases were analyzed in the study of Aigelsreiter et al. (47) and taken over in this study for comparison after re-evaluation of the diagnoses by CL and OS. The histological diagnoses of LCC, SCC, LGDN and HGDN was made according to internationally accepted morphologic criteria and, as described above, by two investigators (CL and OS) in consensus using a multiheaded microscope. (70) Also all HCA and FNH were reevaluated in consensus and the diagnoses confirmed. All cases were evaluated for intracytoplasmic hyaline inclusions, MDB and IHB, on light microscopy and results were recorded.

5.4. Immunohistochemistry

Dewaxed 3 µm thick sections of FFPE tissues were stained with antibodies against K8/18 and p62 as described below. Histological diagnoses of hepatocyte nuclear factor 1A (HNF1A)-inactivated HCA (H-HCA) and inflammatory HCA (I-HCA) types as well as FNH were confirmed by staining with antibodies against glutamine synthetase (GS) and liver fatty acid-binding protein (LFABP) as outlined

below. For all immunohistochemical procedures primary antibodies were omitted and replaced by diluent buffer for negative control.

Immunohistochemistry allows identification and localization of antigens in histological sections. (8, 83) It is a two-step procedure. (83) First a primary monoclonal or polyclonal antibody reacts with the specific antigen. (17, 83) Second specific binding of the primary antibody is visualized directly or indirectly by marker-labelled primary antibody or by binding of a marked secondary to the primary antibody, respectively. (8, 83) If needed, the signal can be amplified by using avidin-biotin complexes. (17, 83)

Keratins 8/18 immunohistochemistry. FFPE sections were incubated at 70°C for 1 hour followed by deparaffinization in xylene and rehydration through ethanol in decreasing concentrations (xylene/100%-100%-90%-80%-50%-phosphate-buffered saline (PBS, pH 7.3)). As recommended by the manufacturer, sections were microwaved for 40 minutes at 150 Watt after placing them in target retrieval solution (pH 9; S2367, Dako, Glostrup, Denmark). After microwaving sections were left to cool down at room temperature for 20 minutes. Following this, sections were washed in cold water and PBS. Endogenous peroxidase activity was blocked by Dako REAL™ peroxidase-blocking solution (S2023, Dako, Glostrup, Denmark) for 10 minutes prior to washing in PBS. Now sections were incubated with primary mouse monoclonal antibodies (both diluted 1:50 in Dako REAL™ antibody diluent (S2022, Dako, Glostrup, Denmark); Keratin 18 Ab-1 (Clone DC10), NeoMarkers, Fremont, California, USA; Cytokeratin 8, Novocastra™ Liquid, Newcastle, UK) at room temperature for 2 hours. Incubation with secondary and tertiary antibodies (Dako REAL™ Detection System, Peroxidase/DAB+, Rabbit/Mouse; K5001, Dako, Glostrup, Denmark) was applied for 30 minutes each in order to assess binding of K8/18. Intermediately, sections were washed in PBS. After applying AEC substrate chromogen (K3464, Dako, Glostrup, Denmark) for 10 minutes, sections were washed in water, counterstained with hematoxylin, washed in hot water and coverslipped with Aquatex® (1085620050, Merck, Darmstadt, Germany), directly out of the water.

P62 immunohistochemistry. FFPE sections were incubated at 70°C for 1 hour followed by deparaffinization in xylene and rehydration through ethanol in decreasing concentrations (xylene/100%-100%-90%-80%-50%-PBS (pH 7.3)). As recommended by the manufacturer, sections were microwaved for 40 minutes at 150 Watt after placing them in target retrieval solution (pH 6; S1699, Dako, Glostrup, Denmark). After microwaving sections were left to cool down at room temperature for 20 minutes. Following this, sections were washed in cold water. Endogenous perioxidase activity was blocked by Dako REAL™ peroxidase-blocking solution (S2023, Dako, Glostrup, Denmark) for 10 minutes. Now sections were washed in wash buffer (S3006, Dako, Glostrup, Denmark) and incubated with primary guinea pig polyclonal antibodies (diluted 1:50 in Dako REAL™ antibody diluent (S2022, Dako, Glostrup, Denmark); GP62-C, Progen, Heidelberg, Germany) at room temperature prior to washing in wash buffer. Incubation with peroxidase-conjugated rabbit anti-guinea pig immunoglobulins (diluted 1:1000 in Dako REAL™ antibody diluent (S2022, Dako, Glostrup, Denmark); P0141, Dako, Glostrup, Denmark) and labelled polymer (EnVision + System-HRP; K5007, Dako, Glostrup, Denmark) was applied for 30 minutes each. Intermediately, sections were washed in wash buffer. After applying AEC substrate chromogen (K3464, Dako, Glostrup, Denmark) for 10 minutes, sections were washed in wash buffer and manually washed in water, counterstained with hematoxylin, washed in hot water and coverslipped with Aquatex® (1085620050, Merck, Darmstadt, Germany), directly out of the water.

GS immunohistochemistry. FFPE sections were incubated at 70°C for 1 hour. GS staining was carried out by Ventana automated slide stainer (Ventana Medical Systems, Inc., Arizona, US). Sections were prepared by applying Cell Conditioning 1 solution (CC1; 950-124, Ventana, Arizona, US) prior to incubation with primary antibodies against GS (diluted 1:5000 in antibody diluent (251-018, Ventana, Arizona, US)) for 32 minutes. For binding assessment ultraView Universal DAB Detection Kit was applied (760-500, Ventana, Arizona, USA) prior to counterstaining with hematoxylin (760-2021, Ventana, Arizona, USA). After the sections have been taken out from the automated slide stainer they were washed in water and Pril (Henkel, Dusseldorf, Germany). Dehydration through ethanol in

increasing concentrations (80%-90%-100%-butyl acetate) was followed by coverslipping with Entellan® (1079610500, Merck, Darmstadt, Germany).

LFABP immunohistochemistry. FFPE sections were incubated at 70°C for 1 hour followed by deparaffinization in xylene and rehydration through ethanol in decreasing concentrations (xylene/100%-100%-90%-80%-50%-PBS (pH 7.3)). As recommended by the manufacturer, sections were microwaved for 40 minutes at 150 Watt after placing them in target retrieval solution (pH 9; S2367, Dako, Glostrup, Denmark). After microwaving sections were left to cool down at room temperature for 20 minutes. Following this, sections were washed in cold water. Endogenous perioxidase activity was blocked by Dako REAL™ peroxidase-blocking solution (S2023, Dako, Glostrup, Denmark) for 10 minutes. Now sections were washed in wash buffer (S3006, Dako, Glostrup, Denmark) and incubated with primary rabbit polyclonal antibodies against LFABP (diluted 1:100 in Dako REAL™ antibody diluent (S2022, Dako, Glostrup, Denmark); ab7807, Abcam, Cambridge, UK) at room temperature prior to washing in wash buffer. Incubation with labelled polymer (EnVision + System-HRP; K5007, Dako, Glostrup, Denmark) for 30 minutes was followed by washing in wash buffer. After applying DAB substrate chromogen (K3464, Dako, Glostrup, Denmark) for 10 minutes, sections were washed in wash buffer and manually washed in water, counterstained with hematoxylin, washed in hot water, dehydrated through ethanol in increasing concentrations (80%-90%-100%-butyl acetate; 1009832511, Merck, Darmstadt, Germany) and coverslipped with Entellan® (1079610500, Merck, Darmstadt, Germany).

5.5. Statistical analysis

Descriptive statistics, absolute and relative frequencies, were calculated using Microsoft Excel. For Chi-squared and Fisher's exact test IBM SPSS Statistics 23 was used.

5.6. Photomicrographs

Photomicrographs have been taken with Nikon Eclipse 80i in combination with a derivate of the Nikon Digital Sight Series.

6. Results

6.1. Histological reevaluation of study cases

Screening of all cases of the HCC cohort yielded 20 LGDN characterized by absence of cytologic atypia, a mildly decreased number of portal tracts and very few unpaired arteries as compared to regenerative nodules (Figure 16 C-D). Regenerative nodules were characterized by a lack of features of cytologic and architectural atypia (Figure 16 A-B). Furthermore, we identified 13 HGDN featuring increased cellularity, small cell type, cytologic atypia, a decreased number of portal tracts and an increased number of unpaired arteries (Figure 17 A-B). In addition, in 7 cases foci of frank HCC were identified within HGDN (Figure 17 C-D, Figure 18).

In addition, from all achieved cases of non-cirrhotic liver resections 13 cases of HCA and 23 cases of FNH were selected for H&E and immunohistochemical analysis based on availability of sufficient material for immunohistochemical analysis. On H&E histology, the diagnosis of HCA was based on the following criteria: Parenchymal mass without portal tracts composed of hepatocytes without cytologic atypia arranged in trabecular structures consisting of 1 to 2 cell layers (Figure 19). HCA cases were typed according to morphological features and the results of immunohistochemical analyses with antibodies against GS and LFABP in I- and H-HCA types. I-HCA (n = 8) showed dilated sinusoids, pseudo-portal tracts (i.e. vessels embedded in fibrous tissue and bordered by ductular-like reaction) and inflammatory infiltrates. H-HCA types (n = 3) exhibited diffuse steatosis. (39, 73)

The diagnosis FNH was assigned to cases with tumors composed of normal hepatocytes in trabecular arrangement forming parenchymal nodules separated by fibrous septa. Within the septa ductular reaction and inflammatory infiltrates but no regular interlobular bile ducts were present (Figure 20). All HCA and FNH were stained with antibodies against GS and LFABP (Figure 21-23). FNH showed map-like reactivity with antibodies against GS and both, H-HCA and I-HCA, were consistently not labelled with these antibodies. While H-HCA were negative for LFABP, I-HCA were positive. 2 HCA cases did not show reactivity with GS or

LFABP antibodies and thus did not fit in either category. These cases were defined as "not otherwise specified" (NOS) HCA in this study.

6.2. Detection of hyaline inclusions in HCC and precursor lesions on H&E histology and immunohistochemistry

H&E histology revealed MDB in HCC as well as in precursors of HCC in cirrhotic liver. MDB were detected as irregularly shaped, hyaline and eosinophilic inclusions within cytoplasm of hepatocytes (Figure 24 A, Figure 25 B). IHB were only present in HCC or in HCC foci of HGDN. They were identified as globular shaped, hyaline and eosinophilic inclusions frequently surrounded by a clear halo (Figure 25 B). On immunohistochemistry MDB were characterized by reactivity with antibodies against K8/18 and p62 (Figure 24 B-C, Figure 25 C-D) whereas IHB showed reactivity with antibodies against p62 only (Figure 25 C-D). Table 7 shows frequency of intracytoplasmic hyaline inclusions on H&E histology and immunohistochemistry in HCC precursors in cirrhotic as well as in non-cirrhotic liver.

Table 7: Frequency of intracytoplasmic hyaline inclusions on H&E- and immunostains. (Own representation)

		H&E stains		Immunostains	
Entity	**n**	**MDB n (%)**	**IHB n (%)**	**MDB n (%)**	**IHB n (%)**
HCC	90	36 (40.0)	28 (31.1)	36 (40.0)	28 (31.1)
RN	61	28 (45.9)	0 (0.0)	33 (54.1)	0 (0.0)
LCC	11	4 (36.4)	0 (0.0)	3 (27.3)	0 (0.0)
SCC	10	1 (10.0)	0 (0.0)	2 (20.0)	0 (0.0)
LGDN	20	4 (20.0)	0 (0.0)	4 (20.0)	0 (0.0)
HGDN	13	7 (53.8)	0 (0.0)	8 (61.4)	0 (0.0)
HGDN & HCC	7	5 (71.4)	2 (28.6)	5 (71.4)	2 (28.6)
FNH	23	0 (0.0)	0 (0.0)	0 (0.0)	0 (0.0)
HCA	13	0 (0.0)	0 (0.0)	0 (0.0)	0 (0.0)

MDB: K8/18+, p62+; IHB: K8/18-, p62+

+/-: Positive/Negative; FNH: Focal nodular hyperplasia; HCA: Hepatocellular adenoma; HCC: Hepatocellular carcinoma; H&E: Hematoxylin and eosin; HGDN: High-grade dysplastic nodule; IHB: Intracellular hyaline body; LCC: Large cell change; LGDN: Low-grade dysplastic nodule; MDB: Mallory-Denk body; RN: Regenerative nodule; SCC: Small cell change

In HCC MDB were found in 36 of 90 cases (40.0%) and IHB were detected in 28 of 90 cases (31.1%) on H&E histology as well as on immunohistochemistry. Highest relative frequencies of MDB on H&E histology were found in high-grade precursor lesions of HCC in cirrhotic liver, in 7 of 13 HGDN (53.8%) and in 5 of 7 HGDN combined with emerging HCC (71.4%). In contrast, only in 1 case of LCC MDB were found on H&E stain while this finding could not be confirmed on p62 and K8/18 immunohistochemistry. In 7 cases, 5 RN, 1 SCC and 1 HGDN, presence of MDB was only detected by immunostaining with antibodies against K8/18 and p62 while they were not found on H&E histology.

Interestingly, IHB were only observed in HCC in 28 of 90 cases (31.1%) and in HCC cells in foci of malignant transformation in HGDN in 2 of 7 cases (28.6%) on H&E histology. These findings were confirmed on immunostains by typical reactivity of IHB inclusions with antibodies against p62 whereas no staining was detected with K8/18 antibodies (Figure 25 C-D).

Chi-squared and Fisher's exact test revealed significant differences in occurrence of IHB among different hepatocellular lesions. IHB are significantly more frequent in HCC than in non-malignant precursor lesions. Neither MDB nor IHB have been observed in any of our HCA and FNH cases. Absence of these inclusions on H&E stain was confirmed by immunostaining with antibodies against K8/18 and p62.

During histopathological analysis we encountered 5 cases with co-existing LGDN, HGDN and HCC within the same patient (Table 8). In 3 cases MDB were found in HGDN respective HCC but not in LGDN or RN of non-neoplastic liver. In none of these cases pre-existing MDB disappeared through hepatocarcinogenesis.

Table 8: Prevalence of MDB in HCC and precursors in individual patients. (Own representation)

	MDB on H&E histology and immunohistochemistry			
Precursor MDB n (%)	**RN** 1 (20.0%)	**LGDN** 1 (20.0%)	**HGDN** 4 (80.0%)	**HCC** 4 (80.0%)
Case 1	0	0	1	1
Case 2	0	0	1	1
Case 3	0	0	0	0
Case 4	0	0	1	1
Case 5	1	1	1	1

Score 0: MDB absent, score 1: MDB present

HCC: Hepatocellular carcinoma; H&E: Hematoxylin and eosin; HGDN: High-grade dysplastic nodule; LGDN: Low-grade dysplastic nodule; MDB: Mallory-Denk body; RN: Regenerative nodule

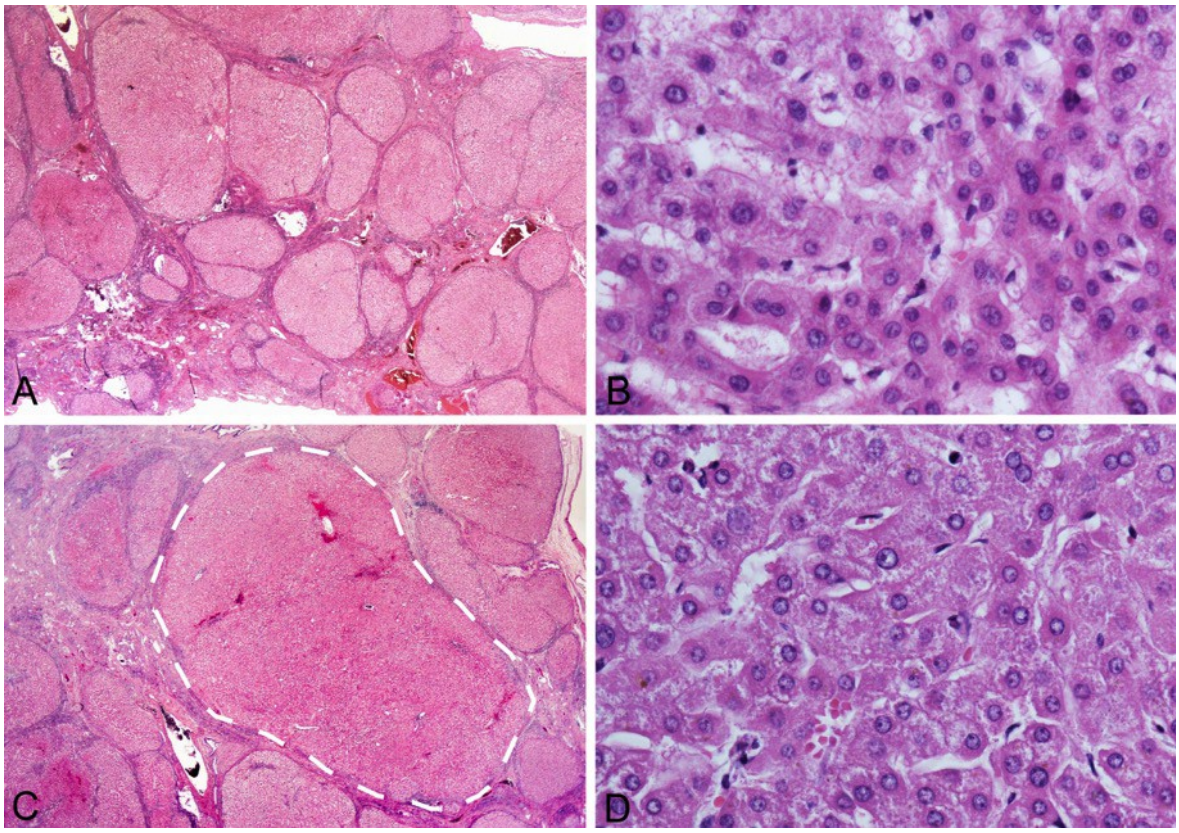

Figure 16: Regenerative nodules (RN, A-B) and low-grade dysplastic nodules (LGDN, C-D)in cirrhotic liver. (A, B) Morphological features of RN. (A) Parenchymal nodules surrounded by fibrous septa (H&E, magnification x10). (B) The liver cells in RN are arranged in regular trabecular structures and lack of cytologic atypia (H&E, magnification x400). (C, D) Morphological features of LGDN. (C) A LGDN (indicated by dashed line) identified by larger size and more intense staining on H&E stain (H&E, magnification x10). (D) The hepatocytes of LGDN show very mild cytologic atypia with slightly increased nucleoli. (H&E, magnification x400). (Own representation)

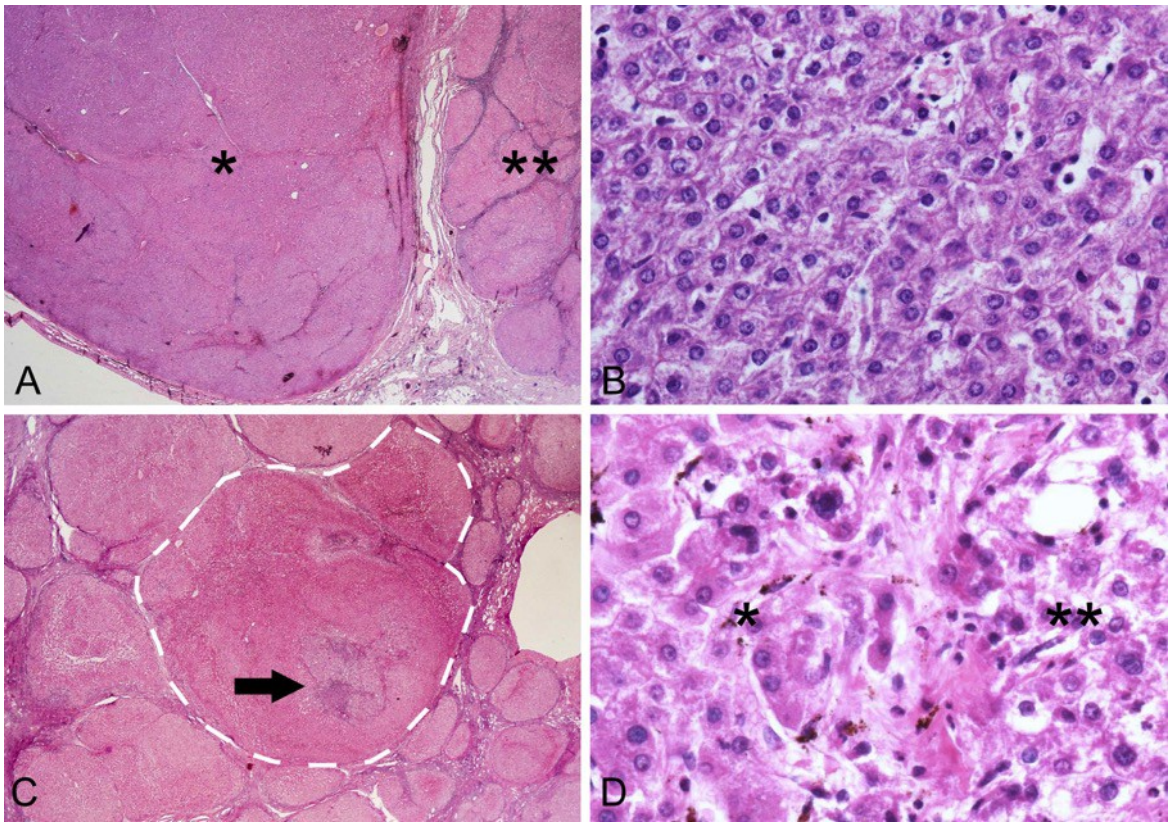

Figure 17: Morphological features of high-grade dysplastic nodule (HGDN, A-B) and HGDN with focal hepatocellular carcinoma (HCC; C-D) in a background of cirrhosis. (A) A HGDN identified by larger size and more intense staining at low magnification (*) as compared to regenerative nodules (; H&E, magnification x10). (B) The hepatocytes of HGDN grow in atypical 2-layered trabecular structures. They are smaller than non-neoplastic hepatocytes and exhibit an increased nuclear to cytoplasmic ratio (H&E, magnification x400). (C) A HGDN with focal malignant transformation. Within the HGDN (indicated by dashed line) a nodule-in-nodule phenomenon is seen (arrow; H&E magnification x10). (D) In higher magnification the HCC cells (**) show high-grade cytologic atypia and invasion in septal fibrous stroma of the HGDN (*) (H&E, magnification x400). (Own representation)**

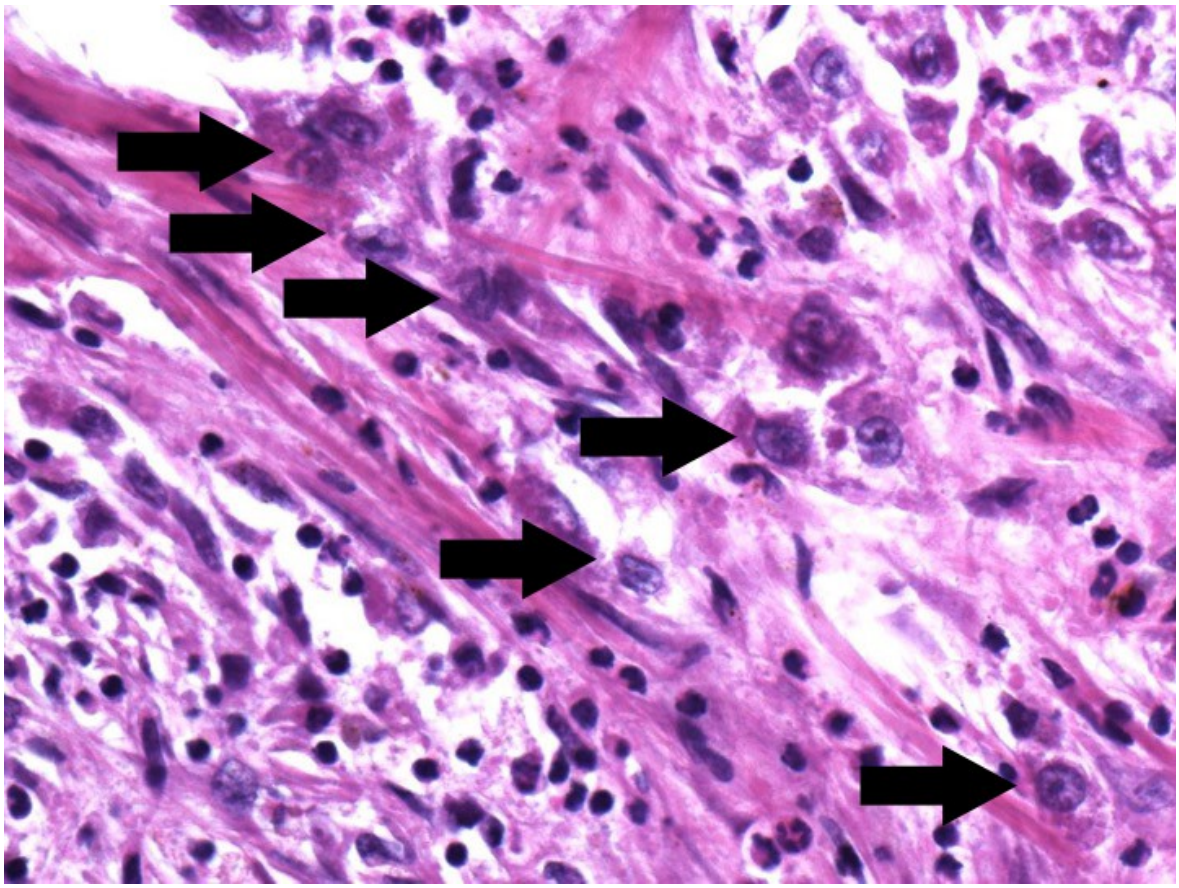

Figure 18: High-grade dysplastic nodule (lower left) with hepatocellular carcinoma (HCC) focus (upper right). HCC cells with high-grade atypia invade septal fibrous stroma (H&E, magnification x600). (Own representation)

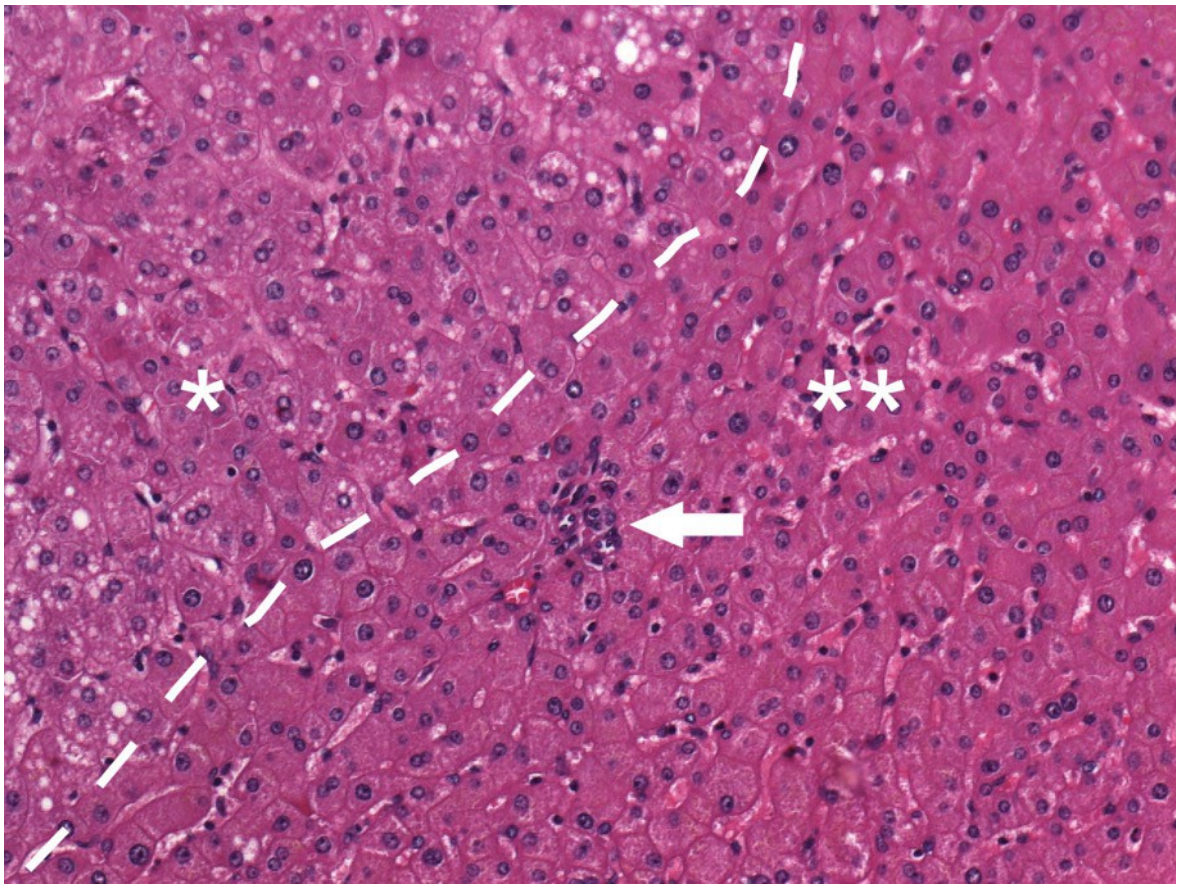

Figure 19: Normal liver parenchyma (**) with a small portal tract (arrow) and hepatocellular adenoma (HCA, *) consisting of hepatocytes without atypia and arranged in trabecular sheets. The HCA cells are slightly larger than normal hepatocytes. They contain large and small vesicular lipid droplets (H&E, magnification x200). (Own representation)

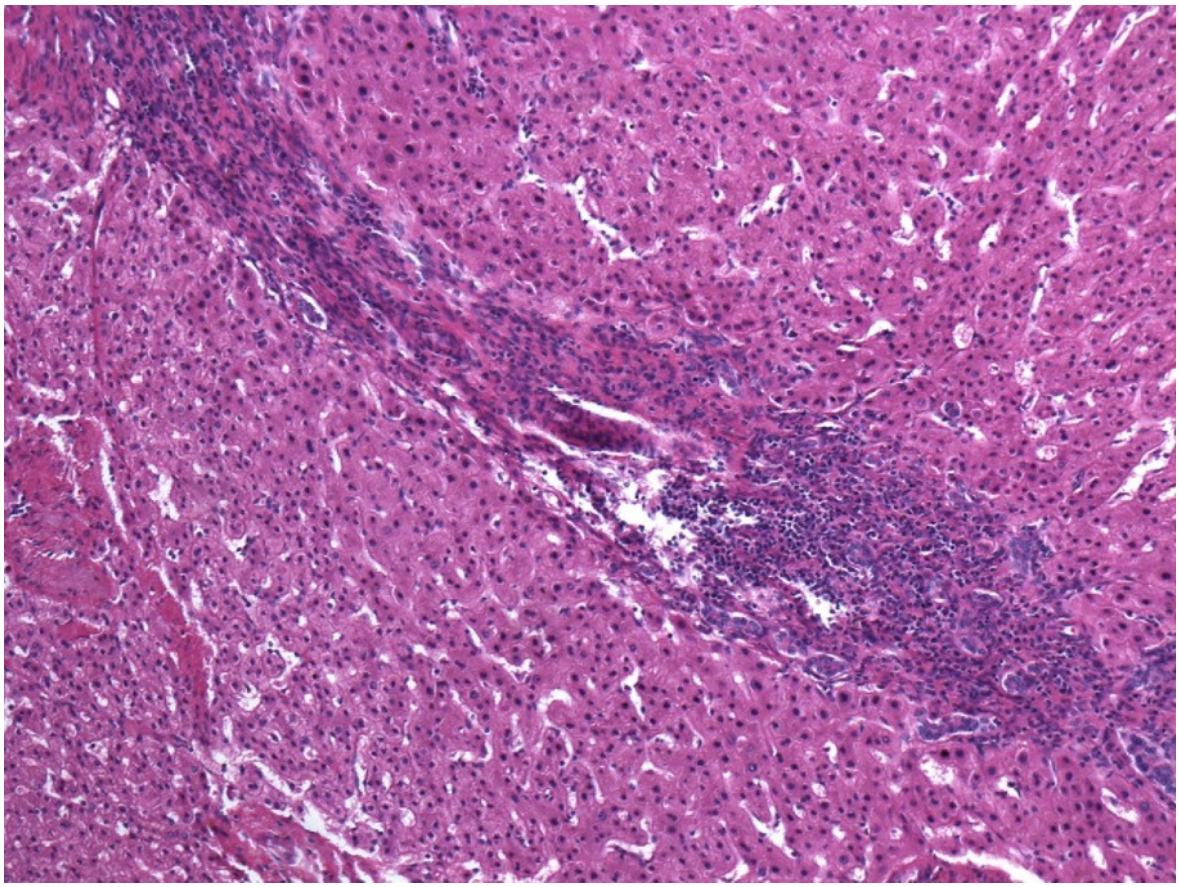

Figure 20: Ductular reaction within a fibrous septum in focal nodular hyperplasia (H&E, magnification x100). (Own representation)

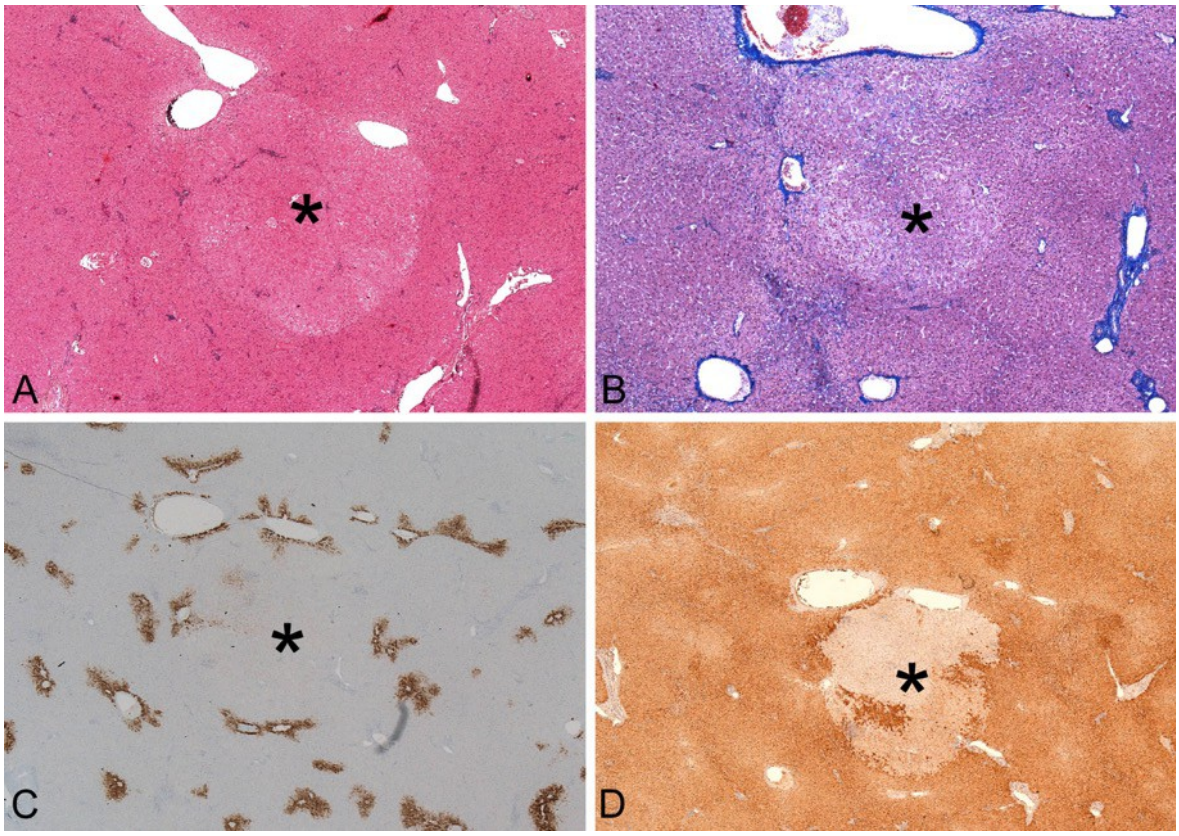

Figure 21: Hepatocyte nuclear factor 1A-inactivated hepatocellular adenoma (H-HCA, *) surrounded by normal liver parenchyma. (A) H-HCA identified by a less intense staining on H&E stain (H&E, magnification x20). (B) Chromotrope-aniline blue (CAB) stain demonstrates lack of cirrhosis in surrounding liver and absence of larger fibrous septa within H-HCA (H&E, magnification x40). (C) H-HCA showing no reactivity with antibodies against glutamine synthetase (GS). The normal liver parenchyma shows perivenular reactivity with GS antibodies (H&E, magnification x20). (D) Loss of liver fatty acid-binding protein (LFABP) expression in the hepatocytes of H-HCA whereas the normal hepatocytes show reactivity with antibodies against LFABP (H&E, magnification x20). (Own representation)

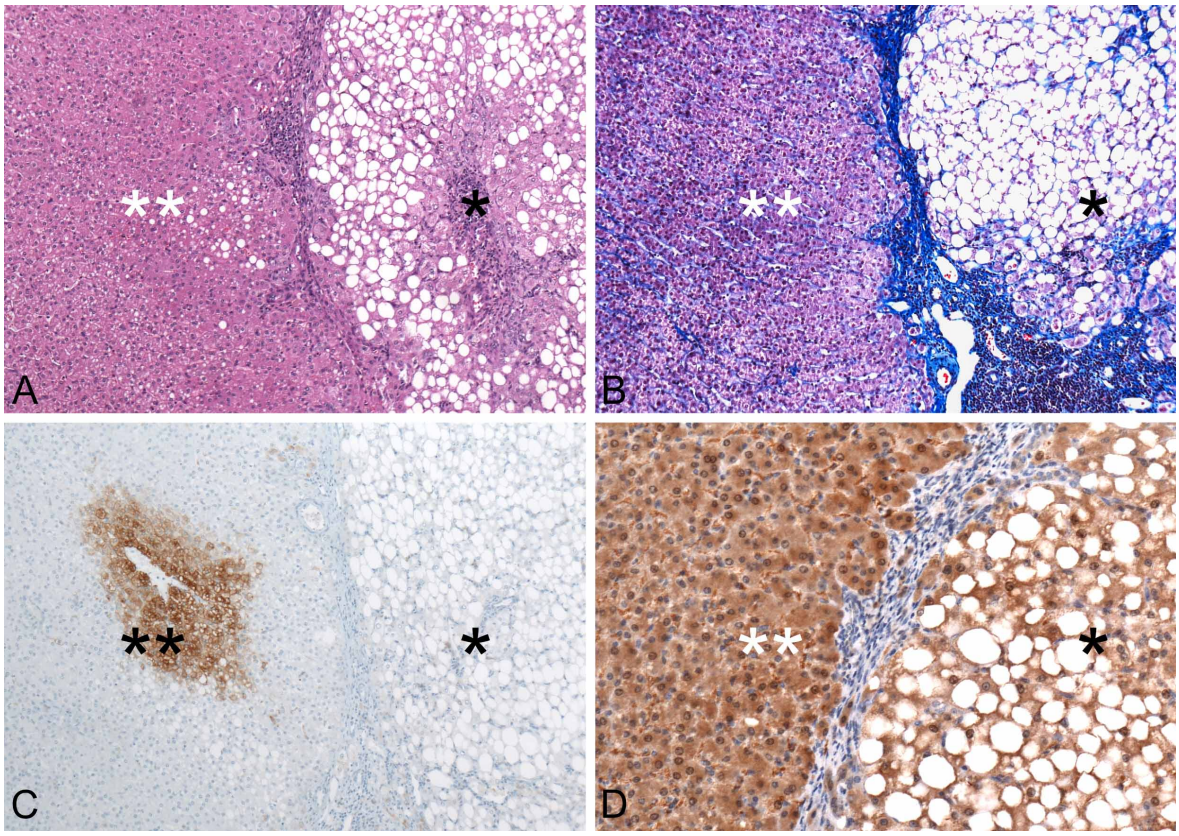

Figure 22: Atypical inflammatory hepatocellular adenoma (I-HCA) with marked steatosis (*) surrounded by normal liver parenchyma (**). (A) I-HCA identified by strong diffuse steatosis, inflammatory infiltrates, sinusoidal dilatation and pseudo-portal tracts (H&E, magnification x40). (B) Chromotrope-aniline blue (CAB) stain demonstrates lack of cirrhosis in surrounding liver (H&E, magnification x100). (C) I-HCA show no reactivity with antibodies against glutamine synthetase (GS). The normal liver parenchyma shows perivenular reactivity with GS antibodies (H&E, magnification x100). (D) Liver fatty acid-binding protein (LFABP) expression is retained in I-HCA as well as in the normal liver (H&E, magnification x200). (Own representation)

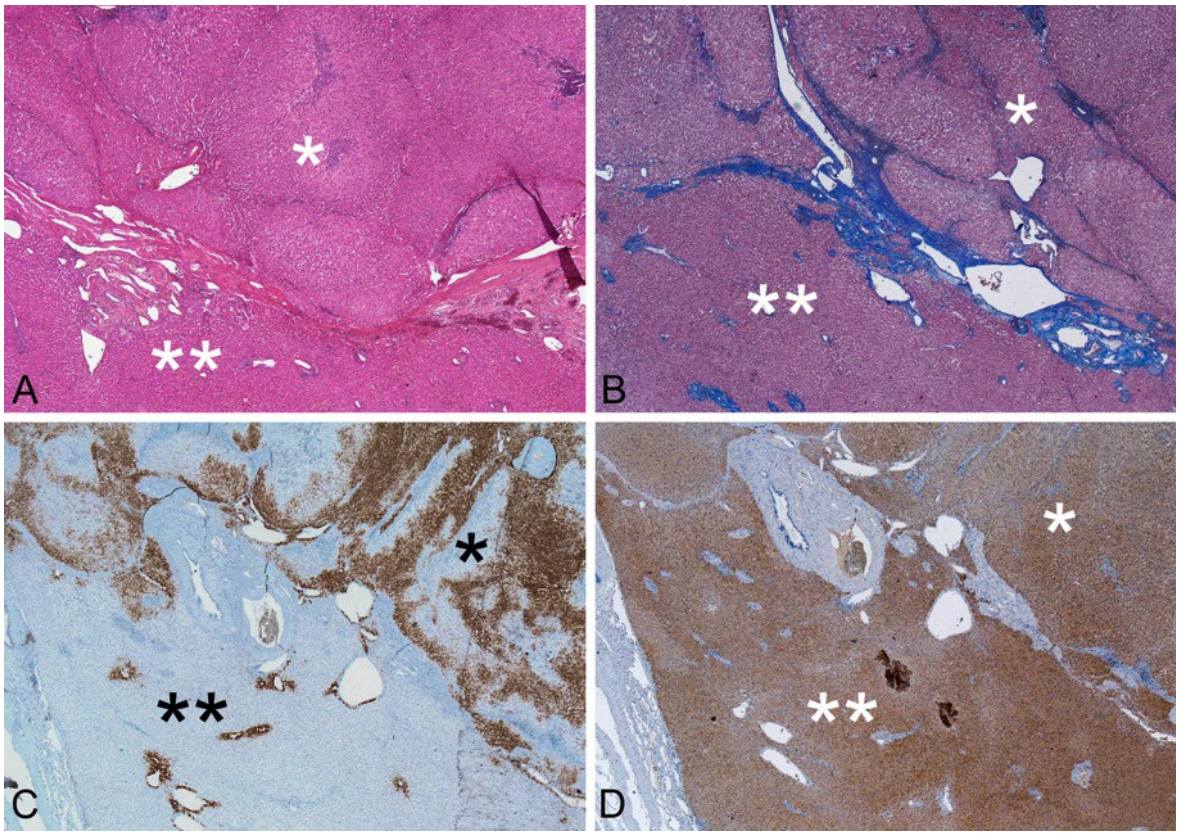

Figure 23: Focal nodular hyperplasia (FNH, *) and adjacent normal liver parenchyma (**). (A) FNH on H&E stain showing parenchymal nodules separated by fibrous septa with ductular reaction (H&E, magnification x20). (B) Chromotrope-aniline blue (CAB) stain of FNH highlighting fibrous septa surrounding parenchymal nodules of varying size (H&E, magnification x20). (C) Glutamine synthetase (GS) stain of FNH demonstrating map-like pattern of FNH. The hepatocytes of the normal liver show perivenular reactivity with antibodies against GS (H&E, magnification x20). (D) Expression of liver fatty acid-binding protein (LFABP) is retained in FNH as well as in the normal liver (H&E, magnification x20). (Own representation)

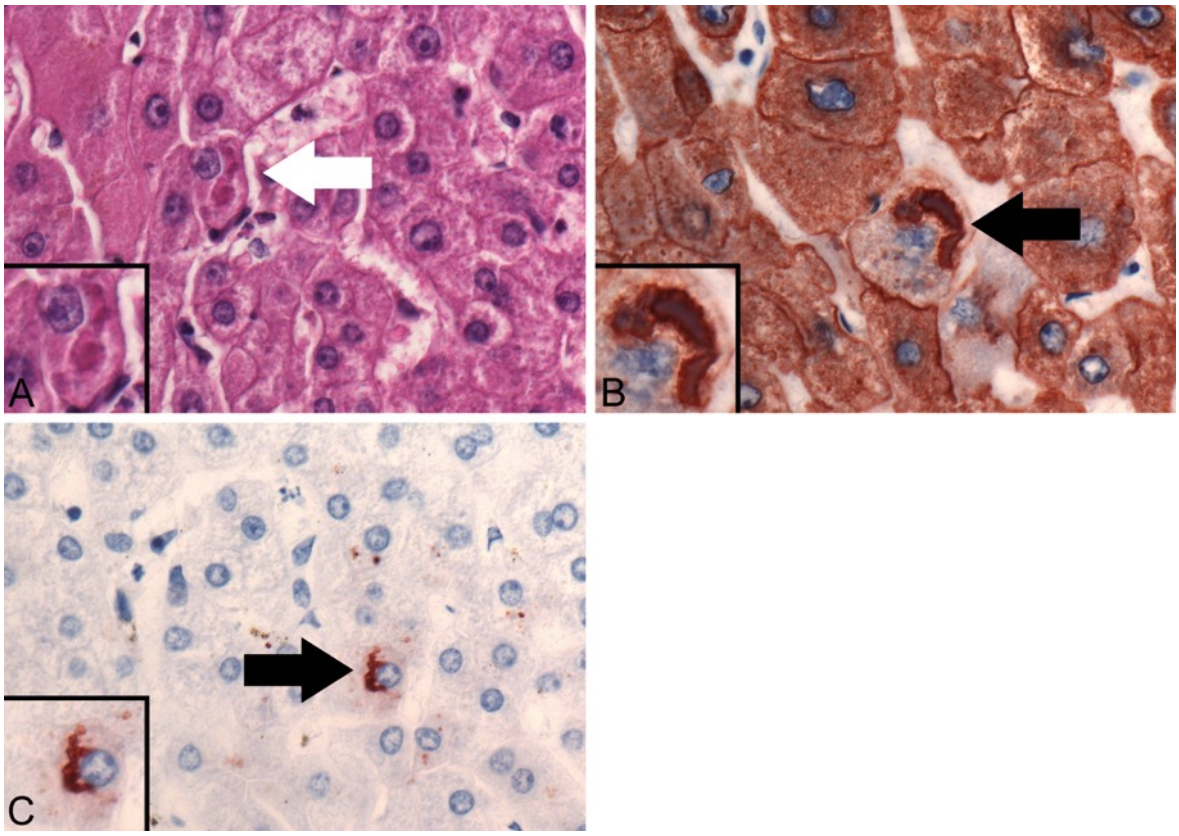

Figure 24: Mallory-Denk body (MDB, arrows) in the cytoplasm of a hepatocyte with small cell change. (A) MDB is seen as an irregular shaped and eosinophilic hyaline cytoplasmic inclusion (higher magnification shown in inset; H&E, magnification x600). (B) MDB is decorated with antibodies against keratins 8/18 (K8/18; arrow, higher magnification shown in inset) whereas the cytoplasm shows significantly decreased reactivity with K8/18 antibodies. Surrounding hepatocytes show regular K8/18 staining (H&E, magnification x600). (C) MDB is also positive with antibodies against p62 (arrow, higher magnification shown in inset; H&E, magnification x600). (Own representation)

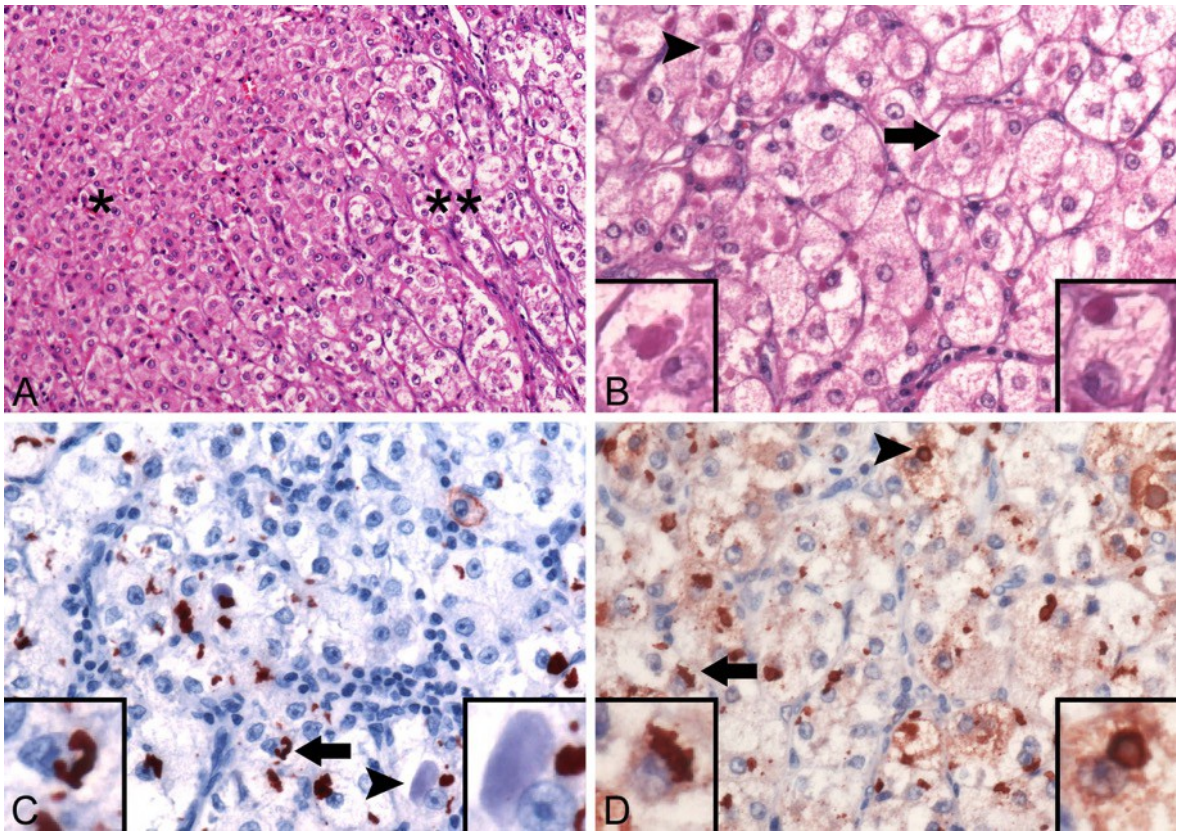

Figure 25: Mallory-Denk bodies (MDB) and intracellular hyaline bodies (IHB) in high-grade dysplastic nodule (HGDN) with hepatocellular carcinoma (HCC) focus. (A) HCC focus (**) within an HGDN (*) on H&E stain. HCC focus is composed of malignant hepatocytes arranged in broad trabecular structures 2 to 4 cell layers wide (right half of figure; H&E, magnification x200). (B) Typical MDB and IHB can be found in cells of HCC focus on H&E stain. The HCC cells show polymorphic nuclei and light cytoplasm. Some of the HCC cells harbor MDB (arrow, higher magnification shown in inset), others show IHB inclusions (arrowhead, higher magnification shown in inset). While MDB are irregularly shaped IHB are globular eosinophilic structures (H&E, magnification x400). (C) MDB (arrow, higher magnification shown in inset) showing reactivity with antibodies against keratins 8/18 (K8/18) while IHB (arrowhead, higher magnification shown in inset) are negative on K8/18 stain (H&E, magnification x200). (D) Both, MDB (arrow, higher magnification shown in inset) and IHB (arrowhead, higher magnification shown in inset) are decorated with antibodies against p62 (H&E, magnification x200). (Own representation)

7. Discussion

HCC is a highly vascularized tumor. (84) The high density of vascular spaces within HCC provides the basis for a radiologic phenomenon called "wash in and wash out" which refers to rapid accumulation and similarly rapid disappearance of contrasting agent in a HCC in cirrhotic liver. (84, 85) This phenomenon exhibits high sensitivity and specifity for the diagnosis of HCC in a background of cirrhosis. (84) It is particularly reliable in HCC of > 2 cm in diameter. (45) Therefore, radiologic imaging with contrasting agents like computed tomography (CT) or magnetic resonance imaging (MRI) are minimal invasive methods that have largely replaced liver biopsy as a diagnostic tool for HCC in patients with cirrhosis. (45, 84) However, tumor biopsy is still required for classification of all nodules occurring in non-cirrhotic liver as well as in larger tumors > 2 cm and smaller tumors < 2 cm in diameter in cirrhotic liver showing atypical features on imaging with contrasting agents on CT and/or MRI. (45, 86)

Small nodules < 2 cm in diameter detected on radiological grounds in cirrhotic liver can have a range of histomorphological differential diagnoses including RN, LGDN, HGDN and well-differentiated HCC. (87, 88) Diagnostic features are necessary for unequivocal classification of these lesions and may not be all contained in a tumor biopsy. Therefore differential diagnosis of nodular liver lesions can represent a challenge even for experienced pathologists. E.g. with respect to prognosis and adequate management the distinction of HGDN or HCA from HCC is particularly important. These tumors may show cytologic and architectural atypia. However, one of the most important morphological features, invasion in portal tracts and/or fibrous septa, may be absent from a tumor biopsy due to sampling error. Therefore, a set of antibodies against proteins prevalent in HCC was proposed as tumor markers assessable by immunohistochemistry which help to confirm or reject the diagnosis of HCC in such settings. Reactivity of lesional cells with 2 out of 3 antibodies against glypican 3, heat shock protein 70 and glutamine synthetase exhibits 70% sensitivity and 100% specifity for the diagnosis of HCC. (30) However, detailed immunohistochemical analyses with many antibodies are costly and may not be available at all pathology institutions.

In contrast to MDB, IHB inclusions have been described in HCC only which suggests that IHB may be morphologic markers of hepatocellular malignancy. However, data about the prevalence of IHB in preneoplastic lesions of HCC are limited. Therefore, the aim of this study was to investigate the prevalence of cytoplasmic hyaline inclusions, MDB and IHB, in a well characterized cohort of HCC and precursors of HCC in non-cirrhotic (HCA and FNH) and cirrhotic (LCC, SCC, LGDN and HGDN) liver.

In our study, we could confirm that IHB are features of malignant transformation since they were only found in some types of HCC and in HCC foci within HGDN. However, in HGDN without malignant transformation and all other types of HCC precursors, FNH, HCA, LCC, SCC, RN and LGDN, IHB were not identified neither on H&E nor on immunohistochemistry. As described by others and confirmed in our study, MDB were present in malignant (HCC and foci of HCC in HGDN) and non-malignant tumors and liver tissues. (31) Interestingly, MDB were found in HGDN and in HCC but not in RN and LGDN occurring in the same liver which may indicate a correlation of MDB with nodular lesions of high-grade dysplasia or HCC. The pathogenesis of hyaline inclusions in cells of hepatocellular differentiation is not known in detail. Results of previous studies of our group suggest that chronic oxidative and other cellular stresses-associated damage to intermediate filament K8 and 18 and other proteins, protein misfolding and overwhelmed mechanisms of autophagy and/or proteasomal degradation are among the main contributors in the pathogenesis. While MDB arise in a background of unbalanced K8 and 18 overexpression and hyperphosphorylation IHB are generated when intermediate filaments are intact and therefore they are devoid of K8/18 but contain p62 and ubiquitin as major components which are also found in MDB. (51) Formation of IHB may be associated with forms of particularly severely deranged differentiation since a correlation with high-grade HCC has been reported. (47)

In our study, IHB have only been found in HCC on light microscopy. It has to be kept in mind that IHB may resemble other intracytoplasmic globular and eosinophilic types of inclusions such as megamitochondria, α1-antitrypsin globules or fibrinogen inclusions. However, these inclusions are mostly negative with p62

and also ubiquitin antibodies. Although the results from our study indicate that both, MDB and IHB, may be detectable with slightly higher sensitivity, immunohistochemistry may not be necessary to confirm or reject the identification of the particular type of hyaline inclusion in many cases.

In summary, owing to their distinct features on H&E histology hyaline inclusions are easy and reliably detectable at no extra cost like for elaborate immunohistochemical marker panels and support the diagnosis of high-grade dysplasia or malignancy. IHB may serve as tumor markers for HCC whereas the presence of MDB in a dysplastic nodule may favor the diagnosis of a high-grade lesion. These simple morphologic features are important inexpensive markers assessable on H&E histology. Pathologists should be aware of these features helpful for both, the classification of nodular liver lesions in tumor biopsies and avoidance of unnecessary cost due to the application of elaborate immunohistochemical marker panels. In this respect, the diagnostic utility of hyaline cytoplasmic inclusions should be investigated in further studies.

8. References

1. Kirsch J. Hepatobiliäres System und Pankreas. In: Bob A, Bob K, editors. Anatomie. 3rd ed. Stuttgart: Georg Thieme Verlag KG; 2014. p. 734-62.
2. Drake RL, Vogl W, Mitchell AW. Gray's Anatomie für Studenten. Paulsen F, editor. München: Elsevier GmbH; 2005.
3. Anderhuber F, Filler TJ, Pera F, Peuker ET. Innere Organe in Thorax, Abdomen und Becken. In: Anderhuber F, Pera F, Streicher J, editors. Waldeyer - Anatomie des Menschen. 19th ed. Berlin: De Gruyter; 2012.
4. Krishna M. Microscopic Anatomy of the Liver. Clinical Liver Disease. 2013;2(S1):4-7.
5. Saxena R. Microscopic Anatomy, Basic Terms, and Elemental Lesions. In: Saxena R, editor. Practical Hepatic Pathology: A Diagnostic Approach. 2nd ed. Philadelphia: Elsevier GmbH; 2018. p. 3-29.
6. Schirmacher P, Dienes H, Jochum W, Trauner M, Lackner C. Leber und intrahepatische Gallenwege. In: Böcker W, Denk H, Heitz PU, Höfler G, Kreipe H, Moch H, editors. Pathologie. 5th ed. München: Elsevier GmbH; 2012. p. 623-66.
7. Hartmann M, Pabst M-A, Dohr G, Schmied R, Caluba H-C. Zytologie, Histologie und mikroskopische Anatomie. Wien: facultas.wuv - Maudrich; 2010.
8. Lüllmann-Rauch R, Asan E. Taschenlehrbuch Histologie. Stuttgart: Georg Thieme Verlag KG; 2015.
9. Chan AW, Quaglia A, Haugk B, Burt A. Atlas of Liver Pathology. New York: Springer-Verlag; 2014. 19-37 p.
10. Bianchi L, Denk H, Stolte M, Walch A, Riede U-N. Hepatopankreatisches System. In: Riede U-N, Werner M, Schaefer H-E, editors. Allgemeine und spezielle Pathologie. 5th ed. Stuttgart: Georg Thieme Verlag; 2004. p. 735-808.
11. Wiegand J, Berg T. The etiology, diagnosis and prevention of liver cirrhosis-part 1 of a series on liver cirrhosis. Dtsch Arztebl Int. 2013;110(6):85-91.
12. Pinzani M, Rosselli M, Zuckermann M. Liver cirrhosis. Best Pract Res Clin Gastroenterol. 2011;25(2):281-90.
13. Blachier M, Leleu H, Peck-Radosavljevic M, Valla D-C, Roudot-Thoraval F. The burden of liver disease in Europe: a review of available epidemiological data. J Hepatol. 2013;58(3):593-608.

14. Zhou W-C, Zhang Q-B, Qiao L. Pathogenesis of liver cirrhosis. World J Gastroenterol. 2014;20(23):7312-24.
15. Silbernagl S, Lang F. Taschenatlas der Pathophysiologie. Stuttgart New York: Georg Thieme Verlag KG; 2013.
16. Hadem J, Manns MP, Caselitz M. Innere Medizin. In: Greten H, Greten T, Rinninger F, editors. Innere Medizin. 13th ed. Stuttgart: Georg Thieme Verlag KG; 2010. p. 796-869.
17. Dombrowski F. Leber. In: Kirchner T, Müller-Hermelink HK, Roessner A, editors. Kurzlehrbuch Pathologie. 12th ed. München: Elsevier GmbH; 2014. p. 403-14.
18. Yeh MM, Brunt EM. Fatty Liver Disease. In: Ferrell LD, Kakar S, editors. Liver Pathology. 39-66. New York: Demos Medical; 2011.
19. Schuppan D, Afdhal NH. Liver cirrhosis. Lancet. 2008;371(9615):838-51.
20. Angeli P, Bernardi M, Villanueva C, Francoz C, Mookerjee RP, Trebicka J, et al. EASL Clinical Practice Guidelines for the management of patients with decompensated cirrhosis. J Hepatol. 2018.
21. Hassan EA, Abd El-Rehim AS, Hassany SM, Ahmed AO, Elsherbiny NM, Mohammed MH. Fungal infection in patients with end-stage liver disease: low frequency or low index of suspicion. Int J Infect Dis. 2014;23:69-74.
22. Herold G. Innere Medizin. Köln: Herold, Gerd; 2015.
23. Kim HJ, Lee HW. Important predictor of mortality in patients with end-stage liver disease. Clinical and Molecular Hepatology. 2013;19(2):105-15.
24. Balogh J VDr, Asham EH, Burroughs SG, Boktour M, Saharia A, Li X, Ghobrial RM, Monsour HP Jr. Hepatocellular carcinoma: a review. J Hepatocell Carcinoma. 2016;3:41-53.
25. Mittal S, El-Serag HB. Epidemiology of HCC: Consider the Population. J Clin Gastroenterol. 2013;47(0):2-6.
26. Li H, Jia J-D. The Relationship between Liver Fibrosis and Hepatocellular Carcinoma. In: Qiao L, Li Y, Yan X, George J, editors. Molecular Aspects of Hepatocellular Carcinoma. 1st ed. Sharja, United Arab Emirates: Bentham Science; 2012. p. 3-7.

27. Reichen J. Leberzirrhose und ihre Komplikationen. In: Pape GR, Göke B, editors. Hepatologie für die Praxis. 1st ed. München and others: Urban & Fischer Verlag/Elsevier GmbH; 2006. p. 145-60.
28. Pinter M, Trauner M, Peck-Radosavljevic M, Sieghart W. Cancer and liver cirrhosis: implications on prognosis and management. ESMO Open. 2016;1(2).
29. Tsochatzis EA, Bosch J, Burroughs AK. Liver cirrhosis. Lancet. 2014;383(9930):1749-61.
30. Galle PR, Forner A, Llovet JM, Mazzaferro V, Piscaglia F, Raoul J-L, et al. EASL Clinical Practice Guidelines: Management of hepatocellular carcinoma. J Hepatol. 2018;69(1):182-236.
31. Theise N, Curado M, Franceschi S, Hytiroglou P, Kudo M, Park Y, et al. Hepatocellular carcinoma. In: Bosman FT, Carneiro F, Hruban RH, Theise ND, editors. WHO Classification of Tumors of the Digestive System. 4th ed. Lyon: International Agency for Research on Cancer; 2010. p. 205-16.
32. Kew MC. Hepatocellular carcinoma in developing countries: Prevention, diagnosis and treatment. World J Hepatol. 2012;4(3):99-104.
33. Dhanasekaran R, Alpna L, Cabrera R. Hepatocellular carcinoma: current trends in worldwide epidemiology, risk factors, diagnosis, and therapeutics. Hepat Med. 2012;4:19-37.
34. Schlageter M, Terracciano LM, D'Angelo S, Sorrentino P. Histopathology of hepatocellular carcinoma. World J Gastroenterol. 2014;20(43):15955-64.
35. Paradis V. Histopathology of Hepatocellular Carcinoma. In: Vauthey J-N, Brouquet A, editors. Multidisciplinary Treatment of Hepatocellular Carcinoma. 1st ed. Berlin Heidelberg: Springer-Verlag; 2013. p. 21-32.
36. Lockwood D, Gotley D. Interaction of Tumor with Host Stroma in Hepatocellular Carcinoma. In: Meadows GG, editor. Integration/Interaction of Oncologic Growth. 15th ed. The Netherlands: Springer-Verlag; 2005. p. 165-76.
37. Jain D. Hepatocellular carcinoma - general.: PathologyOutlines.com website; 2017. Available at: http://www.pathologyoutlines.com/topic/livertumorHCC.html. Accessed July 11th, 2018.

38. Prokop M, van der Molen A. Leber. In: Prokop M, Galanski M, Schaefer-Prokop C, van der Molen A, editors. Ganzkörper-Computertomographie: Spiral- und Multislice-CT. 2nd ed. Stuttgart: Georg Thieme Verlag KG; 2007. p. 431-502.
39. Torbenson M. Biopsy Interpretation of the Liver. Epstein JI, editor. Philadelphia: Wolters Kluwer; 2015.
40. Brunt EM. Histopathologic features of hepatocellular carcinoma. Clin Liver Dis. 2012;1(6):194-9.
41. Liu K, He X, Lei X-Z, Zhao L-S, Tang H, Liu L, et al. Pathomorphological study on location and distribution of Kupffer cells in hepatocellular carcinoma. World J Gastroenterol. 2003;9(9):1946-9.
42. Sugino T, Yamaguchi T, Hoshi N, Kusakabe T, Ogura G, Goodison S, et al. Sinusoidal tumor angiogenesis is a key component in hepatocellular carcinoma metastasis. Clin Exp Metastasis. 2012;25(7):835-41.
43. Leitlinienprogramm Onkologie (Deutsche Krebsgesellschaft DK, AWMF). Diagnostik und Therapie des hepatozellulären Karzinoms. 2013;Langversion 1.0.
44. Fong ZV, Tanabe KK. The clinical management of hepatocellular carcinoma in the United States, Europe, and Asia: a comprehensive and evidence-based comparison and review. Cancer. 2014;120(18):2824-38.
45. Trojan J, Zangos S, Schnitzbauer AA. Diagnostics and Treatment of Hepatocellular Carcinoma in 2016: Standards and Developments. Visc Med. 2016;32(2):116-20.
46. Kinoshita A, Onoda H, Fushiya N, Koike K, Nishino H, Tajiri H. Staging systems for hepatocellular carcinoma: Current status and future perspectives. World J Hepatol. 2015;7(3):406-24.
47. Aigelsreiter A, Neumann J, Pichler M, Halasz J, Zatloukal K, Berghold A, et al. Hepatocellular carcinomas with intracellular hyaline bodies have a poor prognosis. Liver Int. 2016:1-11.
48. Mao Y, Yu F, Wang J, Guo C, Fan X. Autophagy: a new target for nonalcoholic fatty liver disease therapy. Hepat Med. 2016;8:27-37.
49. Glick D, Barth S, Macleod KF. Autophagy: cellular and molecular mechanisms. J Pathol. 2010;221(1):3-12.

50. Dash S, Chava S, Chandra PK, Aydin Y, Balart LA, Wu T. Autophagy in hepatocellular carcinomas: from pathophysiology to therapeutic response. Hepat Med. 2016;8:9-20.
51. Zatloukal K, French SW, Strumptner C, Strnad P, Harada M, Toivola DM, et al. From Mallory to Mallory–Denk bodies: What, how and why? Exp Cell Res. 2007;313(10):2033-49.
52. Liu WJ, Ye L, Huang WF, Guo LJ, Xu ZG, Wu HL, et al. p62 links the autophagy pathway and the ubiqutin–proteasome system upon ubiquitinated protein degradation. Cell Mol Biol Lett. 2016;21(29).
53. Umemura A, He F, Taniguchi K, Nakagawa H, Yamachika S, Font-Burgada J, et al. p62, Upregulated during Preneoplasia, Induces Hepatocellular Carcinogenesis by Maintaining Survival of Stressed HCC-Initiating Cells. Cancer Cell. 2016;29(6):935-48.
54. Bao L, Chandra PK, Moroz K, Zhang X, Thung SN, Wu T, et al. Impaired Autophagy Response in Human Hepatocellular Carcinoma. Exp Mol Pathol. 2014;96(2):149-54.
55. Cohen-Kaplan V, Ciechanover A, Livneh I. p62 at the crossroad of the ubiquitin-proteasome system and autophagy. Oncotarget. 2016;7(51):83833-4.
56. Strnad P, Zatloukal K, Strumptner C, Kulaksiz H, Denk H. Mallory-Denk-bodies: lessons from keratin-containing hepatic inclusion bodies. Biochim Biophys Acta. 2008;1782(12):764-74.
57. Kanel GC. Drug- and Toxin-induced Liver Diseases. In: Kanel GC, editor. Pathology of Liver diseases. 1st ed. Hoboken, NJ: Wiley Blackwell; 2017. p. 215-30.
58. Theise N. Histopathology of alcoholic liver disease. Clin Liver Dis. 2013;2(2):64-7.
59. Brunt EM, Kleiner DE. When is it NAFLD and when is it ALD?: Can the histologic evaluation of a liver biopsy guide the clinical evaluation? In: Williams R, Taylor SD, editors. Clinical Dilemmas in Non-Alcoholic Fatty Liver Disease. 1st ed. New York: Wiley Blackwell; 2016. p. 72-81.
60. Chelliah AR, Radhi JM. Hepatocellular Carcinoma with Prominent Intracytoplasmic Inclusions: A Report of Two Cases. Case Reports Hepatol. 2016;2016.

61. Jakate S, Giusto D. Hepatocellular Carcinoma Variants. In: Ferrell LD, Kakar S, editors. Liver Pathology. 4th ed. New York: Demos Medical; 2011. p. 407-30.
62. Suriawinata AA, Thung SN. Liver Pathology: An Atlas and Concise Guide. New York: Demos Medical; 2011.
63. Chan ES, Yeh MM. Cytoplasmic Globules. In: Ferrell LD, Kakar S, editors. Liver Pathology. 4th ed. New York: Demos Medical; 2011. p. 243-50.
64. Wong C, Ng IOL. Genomics of Hepatocellular Carcinoma. In: Gu J, editor. Primary Liver Cancer: Challenges and Perspectives. 1st ed. Berlin Heidelberg: Springer-Verlag; 2012. p. 45-78.
65. Niu Z-S, Niu X-J, Wang W-H, Jing Z. Latest developments in precancerous lesions of hepatocellular carcinoma. World J Gastroenterol. 2016;22(12):3305-14.
66. Roncalli M, Terracciano L, Di Tommaso L, David E, Colombo M. Liver precancerous lesions and hepatocellular carcinoma: The histology report. Digestive and Liver Disease. 2011;43(4):361-72.
67. Park YN. Update on precursor and early lesions of hepatocellular carcinomas. Arch Pathol Lab Med. 2011;135(6):704-15.
68. Hytiroglou P. Morphological Changes of Early Human Hepatocarcinogenesis. Semin Liver Dis. 2004;24(1):65-75.
69. Prodromos H. Hepatitis B. In: Saxena R, editor. Practical Hepatic Pathology: A Diagnostic Approach. 2nd ed. Indianapolis: Elsevier GmbH; 2018. p. 211-22.
70. Neoplasia ICGfH. Pathologic Diagnosis of Early Hepatocellular Carcinoma: A Report of the International Consensus Group for Hepatocellular Neoplasia. Hepatology. 2009;49(2):658-64.
71. Assarzadegan N. Low grade dysplastic nodule: PathologyOutlines.com website; 2017. Available at: http://www.pathologyoutlines.com/topic/livertumorlowgradedysplasticnod.html. Accessed January 25th, 2018.
72. Kwok WY, Hagiwara S, Nishida N, Watanabe T, Sakurai T, Ida H, et al. Malignant Transformation of Hepatocellular Adenoma. Oncology. 2017;92(1):16-28.

73. Roncalli M, Sciarra A, Di Tommaso L. Benign hepatocellular nodules of healthy liver: focal nodular hyperplasia and hepatocellular adenoma. Clin Mol Hepatol. 2016;22(2):199-211.
74. Stoot JH, Coelen RJ, de Jong MC, Dejong CH. Malignant transformation of hepatocellular adenomas into hepatocellular carcinomas: a systematic review including more than 1600 adenoma cases. HPB (Oxford). 2010;12(8):509-22.
75. Vijay A, Elaffandi A, Khalaf H. Hepatocellular adenoma: An update. World J Hepatol. 2015;8(7):2603-9.
76. Nault J-C, Zucman-Rossi J. Genetics of hepatocellular carcinoma: the next generation. J Hepatol. 2014;60(1):224-6.
77. Ducatman BS. Liver. In: Cibas ES, Ducatman BS, editors. Cytology: Diagnostic Principles and Clinical Correlates. 4th ed. Philadelphia: Elsevier GmbH; 2014. p. 375-98.
78. Brunt EM, Neuschwander-Tetri BA, Burt AD. Fatty liver disease: alcoholic and non-alcoholic. In: Burt AD, Portmann BC, Ferrell LD, editors. MacSween's Pathology of the Liver. 6th ed. London: Churchill Livingstone 2012. p. 293-360.
79. Petsas T, Tsamandas A, Tsota I, Karavias D, Karatza C, Vassiliou V, et al. A case of hepatocellular carcinoma arising within large focal
nodular hyperplasia with review of the literature. World J Gastroenterol. 2006;12(40):6567-71.
80. Venturi A, Piscaglia F, Vidili G, Flori S, Righini R, Golfieri R, et al. Diagnosis and management of hepatic focal nodular hyperplasia. J Ultrasound. 2007;10(3):116-27.
81. Wee A, Sampatanukul P, Jhala N. Cytohistology of Focal Liver Lesions. Geisinger KR, Pitman MB, editors. Cambridge: Cambridge University Press; 2014.
82. Aigelsreiter A, Pixner T, Denk H, Lackner C. Mallory-Denk-Body-like cytoplasmic inclusions in the cholangiocarcinoma component of a case of combined hepatocellular and cholangiocarcinoma. Virchows Arch (2009). 2009;455(1):201.
83. Moch H, Zimmermann D, Probst-Hensch N. Pathologie: Aufgaben und Methoden. In: Böcker W DH, Heitz PU, Höfler G, Kreipe H, Moch H, editor. Pathologie. 5th ed. München: Elsevier GmbH; 2012.

84. Tan M, Chapman WC. Surgical Diseases of the Liver. In: Klingensmith ME, Chen LE, Glasgow SC, Geoers TA, Melby SJ, editors. The Washington Manual of Surgery. 5th ed. Philadelphia: Wolters Kluwer; 2008. p. 251-63.
85. Bargellini I, Battaglia V, Bozzi E, Lauretti DL, Lorenzoni G, Bartolozzi C. Radiological diagnosis of hepatocellular carcinoma. J Hepatocell Carcinoma. 2014;1:137-48.
86. Jain D. Tissue Diagnosis of Hepatocellular Carcinoma. J Clin Exp Hepatol. 2014;4(3):67-73.
87. Gheonea I-A, Streba CT, Cristea CG, Stepan AE, Ciurea ME, Sas T, et al. MRI and pathology aspects of hypervascular nodules in cirrhotic liver: from dysplasia to hepatocarcinoma. Rom J Morphol Embryol. 2015;56(3):925-35.
88. Di Martino M, Anzidei M, Zaccagna F, Saba L, Bosco S, Rossi M, et al. Qualitative analysis of small (≤2 cm) regenerative nodules, dysplastic nodules and well-differentiated HCCs with gadoxetic acid MRI. BMC Med Imaging. 2016;16:62.